Non-linear behaviour for naturally fractured carbonates and frac-stimulated gas-shales

Nick Barton, NB&A, Oslo, Norway

ABSTRACT

Gas-shales and naturally fractured reservoirs usually produce from several kilometers depth, with fracing-stimulation and eventual water-drive respectively. Due to porosity, the matrix is generally weaker than is typical for basement rocks. The potential pore pressure reduction of 10's of MPa during the early life of the fields, may therefore be a significant proportion of the strength of the matrix. Inevitable non-linear rock strength behaviour for the matrix should not then be ignored. It is therefore unrealistic to utilize a linear Mohr-Coulomb strength criterion as so frequently seen. The joints or natural fractures in the shales and carbonates, which are so important for production, will have producing fracture sets with different roughness and aperture, and few of them are planar enough to follow the frequently used linear Mohr-Coulomb behaviour. Non-linearity especially applies to the favourable shear strength-dilation-permeability coupling which is relevant for both NFR and gas-shales, and to the less desirable stress-closure-permeability coupling of a stress-sensitive reservoir. Non-linear constitutive modelling, partly based on the joint- or fracture-roughness coefficient (JRC) used widely in rock mechanics, also applies to the conversion from hydraulically interpreted theoretical smooth-wall apertures (e) to the larger and non-planar-non-smooth-wall physical apertures (E) through which the oil or gas actually flows to the wells. Simple index tests which can also be applied on joints or fractures recovered in occasional and inevitably expensive core, and which can also be estimated when mapping fractured pavement analogues, have been available in rock mechanics for several decades. They were already incorporated in coupled distinct element (jointed) non-linear modelling routines in 1985. However their implementation in petroleum industry geomechanics seems to be very rare judging by numerous workshops attended in the last seven to eight years on both sides of the Atlantic. Application of non-linear (non Mohr-Coulomb) rock mechanics, using recovered core from Ekofisk in 1986-1987 in order to model fracture shear-dilation coupling with simplified E and e tracking during compaction, may be the earliest example. Remarkably, these more realistic applications seem to be rare.

DEFINITION OF COMMON ROCK MECHANICS TERMS. *(NOTE THAT FIRST BREAK HAS NOT YET LISTED ROCK MECHANICS AS ONE OF ITS THOUSANDS OF KEY WORDS).*

PARAMETER	DEFINITION
c	The cohesive strength of intact rock (assuming linear Mohr-Coulomb strength envelopes). A non-linear alternative is proposed.
φ	The frictional strength of intact rock (assuming linear Mohr-Coulomb strength envelopes). A non-linear alternative is proposed.
JRC, JRC_n	Joint- or fracture-roughness coefficient (typical range 0 to 20 from completely smooth-planar to rough-undulating). Scale-dependent. The block-size scaled-value of JRC_n has lower values. See Fig.8.

JCS JCS_n	Joint- or fracture wall strength (typical range 10 to 150 MPa from weak-porous to hard non-porous rock). Scale-dependent. Experience with gas-shales suggests the need for brittle behaviour (also meaning higher JCS) lasting as long as possible, while effective stresses are low enough to prevent the brittle-ductile transition being reached.
r, R	Schmidt-hammer rebound (mean of *top* 50% of tests) on respectively the saturated joint or fracture wall, and on the dry unweathered rock. The ratio r/R describes the degree of fracture-surface weathering/alteration.
L_0 and L_n	Nominal laboratory-sample length, and *in situ* block size or spacing of cross-joints (cross-fractures). In case of anisotropic fracture spacings, tabular block shapes may require two estimates of L_n.
φ_r	Residual friction angle of a joint or fracture after a significant amount of shearing. Ultimate strength is reached earlier, at the end of a shear test. (Typical range of minimum φ_r is 24° to 34°).
$JRC_{mobilised}$	The shear-displacement-dependent mobilization (and post-peak degradation) of the joint roughness coefficient. A widely applicable dimensionless model is illustrated in Figure 15. This demonstrates that frictional strength is not so elementary as single (peak values) of μ = 0.6, 0.85 etc. as pioneered long ago by Byerlee and also widely used today in USA.
δ and δ_{peak}	The ongoing shear displacement, and the shear displacement needed to reach *peak* shear strength, which reduces to < 1% of *in situ* block length when block-size exceeds approximately 100 mm.
σ', σ_1, σ_3, and σ_n'	Effective stress, axial (major) stress, confining (minor) stress, and normal effective stress across a joint or fracture.
K_n and K_s	Normal and shear stiffness of joints or fractures. Both are stress-dependent and non-linear. K_s is also block-size dependent (it is fortunately lower in situ). The ratio Kn/Ks may be from 10 to 100.
Q-value, Jr, Ja	These terms have been used in the world of tunneling for the last 40 years, describe rock mass quality, joint roughness and joint alteration or clay-filling. Q correlates to the stress-dependent static deformation modulus E_{mass} (resembling $Q_{P\ seismic}$ if in GPa), and to the stress-dependent P-wave velocity V_P (see Barton, 2006, 2007c). Q_{H2O} approximates the depth dependent permeability of a rock mass. Usual range in top 1 km is 10^{-4} to 10^{-10} m/s.

INTRODUCTION

In the EAGE workshop on *Naturally Fractured Reservoirs in Real Life*, held in Muscat, Oman in December 2013, Price and Wei (2013) from Shell reported on the conclusions from retrospective analyses of eight case studies of fractured reservoirs, mostly related to carbonate reservoirs in Oman. Through extensive fracture network modelling by a large team of company collaborators, the authors identified the most important factors which they considered necessary for *improved history matching*. A production and forecast time-scale of 10 to 40 years was considered in this extensive study by Shell.

Their list of important factors, including their own verbal additions given during their lecture, included the following: *fracture volume, fracture density, fracture clusters, permeability anisotropy due to stress,* and *aperture sensitivity to stress*. Most of these factors would seem to be amenable to realistic conceptual modelling, using rock mechanics principles and available non-linear methods. Such modelling would obviously need to be made at reduced scale at first, using coupled-process distinct element methods, such as the two-dimensional distinct element (jointed) model UDEC-BB (with non-linear Barton-Bandis joint behaviour), or the three-dimensional model 3DEC-MC (with less realistic linear Mohr-Coulomb joint behavior). The detailed behavioural trends thus revealed would subsequently need to be *up-scaled but not lost*, ready for potentially improved reservoir simulator modelling.

GEOMECHANICS AND FRACTURE CHARACTERIZATION IS DONE DIFFERENTLY IN ROCK MECHANICS

Based on presentations made in the Muscat fractured reservoir workshop, and based on presentations made in several similar workshops and courses attended on both sides of the Atlantic in the last seven to eight years, the writer has gained the strong impression that *geomechanics,* complex enough as it is, seems to be mostly practiced in the petroleum industry without considering the *non-linear* shear strength, dilation, stiffness of the different fracture sets. Much of reality is lost if this is true.

The desirable non-linear *shear-dilation-permeability* coupling and the less desirable and very non-linear fracture *aperture-closure* of a stress-sensitive reservoir, due to effective stress change during production, are also apparently not yet a part of open-source petroleum *geomechanics* literature. The aperture-closure would oppose the assumed benefits of major fracture sets ‘always’ being parallel to the major principal stress, and therefore ‘open’, as often assumed in geophysicist’s analyses of shear wave splitting. In practice the minimum stress may close these assumed conducting features, unless they are with ‘minerally-frozen’ and therefore have channeled-apertures (e.g. Laubach et al. 2004).

Sometimes there is significant deviation from this ‘parallel to major stress’ assumption, due to tectonic influences and the effects of shearing: see Barton (2007) and Barton (2013a). In fact it has been known for many decades that shearing is important for production from carbonate reservoirs, for instance at Ekofisk as described from Norwegian studies in Barton et al. (1986, 1988), and more generally the importance of shear stress was described in the USA by Christine Barton et al. (1995), Townend and Zoback (2001) and by Fairhurst (2013). In the last decade, *fracture shearing* as a result of fracing in gas-shales has to be considered the probable most important and ‘wider-radius’ result of fracing. The impermeable shales

cannot produce without the wider-reaching fracture deformation, especially shearing, according to microseismic evidence, stretching well beyond the central 'ellipsoidal' propped artificial tension fracture region. See for instance Fisher and Warpinski. (2011) and Dusseault (2013).

Also based on workshops attended it is evident that the commonly used term *fracture characterization* as used in the petroleum industry is rather different from the term *fracture characterization* used in rock mechanics for civil or nuclear waste isolation engineering. In rock mechanics, the relative roughness of the fracture sets would be described using JRC (= joint roughness coefficient) and using the wall strength JCS (= joint wall compressive strength) of the different fracture sets. These simply obtained parameters would be an automatic additional focus of attention, and would provide important quantitative abilities to include non-linear shear strength, dilation and eventual aperture closure estimation, as a supplement and clear improvement to what appear to be *typical* present-day petroleum geomechanics routines. (The commonly used terms JRC and JCS, used for several decades in rock mechanics, with thousands of citations, will be demonstrated later).

Fracture characterization as practiced in petroleum geomechanics, seems typically to neglect these widely used rock mechanics terms. However they are actually needed for the non-linear modelling of fracture deformation and its coupling with permeability changes. This part of 4D behaviour, which is more sophisticated than merely 'stress and strain' as sometimes assumed in the geophysics literature, may therefore be poorly interpreted. Non-linear behaviour is inevitable when fractures are involved, as we will see in subsequent figures.

Judging by what has been seen in numerous workshops on both sides of the Atlantic, few petroleum companies appear to be focused on non-linear *rock mechanics understanding and application* in their fractured (or stimulated) reservoir modelling. The methods to be described here are of course amenable to application on reservoir core, such as that applied long ago at Ekofisk, which was referred to earlier. In practice the methods to be described can also be applied when characterizing analogue fractured pavements and cliffs, i.e. by suitable analysis of vertical or oblique drone photography of the pavements or cliffs.

EAGE's president recently expressed her intent of focusing EAGE activities in the next two years on 'Making a difference on a global scale by narrowing the gap'. Her expressed purpose was *narrowing the gap* between geoscience and engineering disciplines. On a modest scale, this article tries to support these important and potentially oil-and-gas producing objectives.

THE SHEAR STRENGTH OF INTACT ROCK MAY BE HIGHLY NON-LINEAR

Petroleum production tends to occur from reservoirs typically several kilometers deep, and from rocks with significant porosity and therefore reduced strength in relation to basement rocks of low porosity. Here one can think of the principally occurring and producing sandstones, carbonates (including chalk) and stimulated oil-shale / gas-shale reservoirs, plus the well fractured-and-faulted basement reservoirs in altered granites, whose productive fractures have very high porosity, despite the usually misleadingly low average porosity, which is often < 1%. Figure 1 shows the non-linearity of dry carbonate rocks, over a large range of stress. Non-linearity will

also occur over the lower range of reservoir stresses, since many tens of MPa are involved during the hoped-for life of the producing reservoir.

It can be highly unrealistic to assume linear Mohr-Coulomb ($c + \sigma' \tan \varphi$) strength envelopes, when large potential increases in effective stress occur, perhaps ranging from 20 to 40 MPa, as a result of production. (Note: c = cohesional strength, φ = frictional strength, and σ' is the effective stress: see page 1). Furthermore, the relationship between conjugate-fracture intersection angles must be expected to change radically, when progressing from a near-surface pavement or cliff, to fractured reservoir depths of several kilometers.

Both of these aspects are illustrated in Figure 2, and also in Figure 3. As pointed out by Barton and Pandey (2011) and a few others in the past, it is also unrealistic and often incorrect to add 'c' and '$\sigma_n' \tan \varphi$', as if these Coulomb shear strength components are mobilized at the same strain. See Barton (2011) for further discussion of this important topic, which was raised more than 50 years ago, in the early days of rock mechanics by Müller (1966).

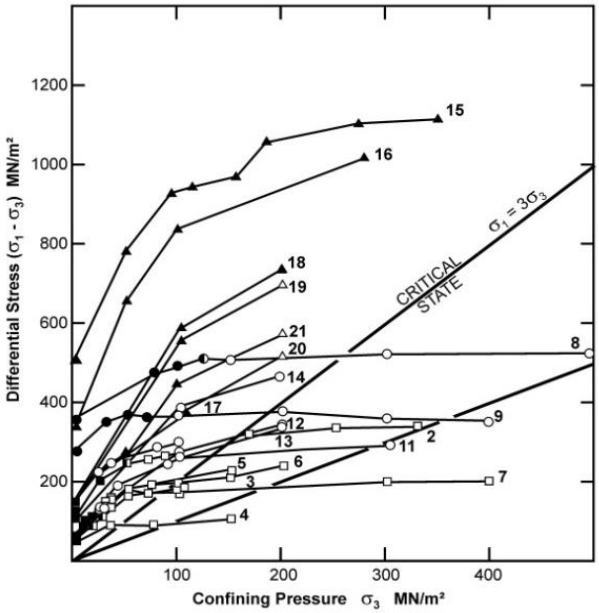

Figure 1 A wide-ranging review of the shear strength of intact rock reported by Barton (1976), included this data set from Mogi (1966).These high-pressure triaxial tests on dry carbonate rocks, and numerous other data from Byerlee (1968) gave the writer the idea of a 'critical state' approach to shear strength limits. The critical state line added by the writer, has a gradient of $\tan^{-1} 1/2$, or 26°.The explanation of this term will become clearer in Figure 2.

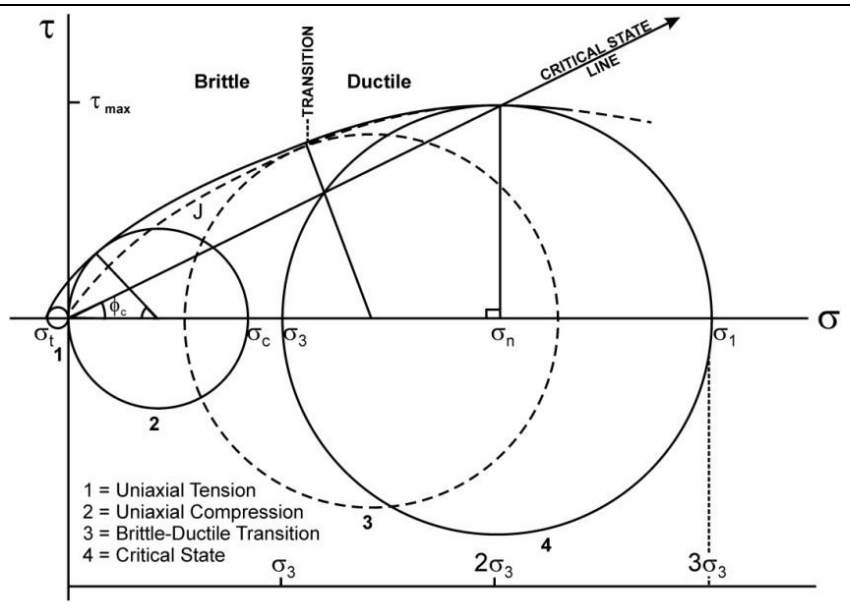

Figure 2 The critical state concept suggested by Barton (1976).This has recently been used by Singh et al. (2011) to derive the equations giving the correct deviation from linear Mohr-Coulomb. A few triaxial tests at low confinement give the complete strength envelope. An especially interesting result of their study was that a majority of rock types have $\sigma_{3\ (critical)} \approx \sigma_c$. In other words Mohr circles #2 and #4 are touching or nearly touching, as indeed illustrated in Figures 2 and 3. Note the intermediate stress-circle #3 representing the brittle-ductile transition. This may be reached as effective stresses increase in the weaker reservoir rocks like chalk and shale. Water flooding would be needed well before this damaging stage.

The maximum possible shear strength operating when the strength envelope becomes horizontal at the critical state, is expressed as: $\sigma_{1\ (max)} = 3\ \sigma_{3\ (critical)}$. The actual closeness of the uniaxial compression (#2) and critical state Mohr circles (#4) was discovered by Singh et al. (2011). The marked superiority of their 2011 'Singh-Singh' criterion, which also caters for poly-axial stress states, was recently confirmed by subsequent review work presented by an independent group: see Shen et al. (2013), who were presenting a 'competing' but less well-fitting intact rock strength criterion of their own, using the results from more than 1,300 triaxial tests.

Note that the brittle-ductile transition shown in Figure 2 is reached at an intermediate confining stress, and there is reason to believe that this will be reached in weaker reservoir rocks such as chalk, and perhaps in weaker (more clay-bearing) shales as effective stresses increase. However pore collapse is a complicating factor in the case of chalk, and a further source of non-linearity.

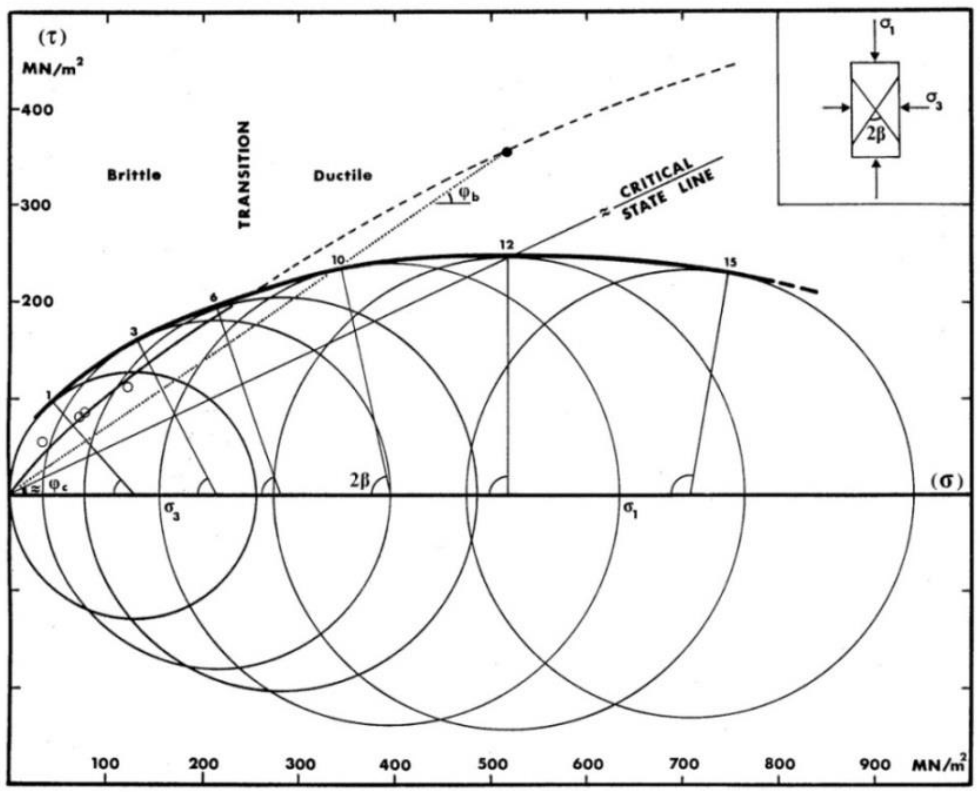

Figure 3 A complete set of Mohr circles for high-pressure tests on strong (UCS = 250 MPa) limestones derived from Byerlee (1968) data reproduced by Barton (1976). The small numbers next to the strength envelope refer to specific triaxial test numbers. Note the addition of the critical state line. Note also the progression of the conjugate-fracture angle 2β towards 90° with increasing depth or confinement. The small circles represent the peak strength of fractures, and the dotted curved envelope, drawn into the inadmissible area for reasons of clarity, was used to demonstrate the maximum empirical strength of (rough) rock fractures, as shown in Figure 4.The potentially / likely strong non-linearity should not be ignored when producing from a reservoir in weaker, more porous carbonates (or shales) with a possible life-time 20-40 MPa change of effective stress. Just the first three Mohr circles define a non-linear envelope, even with this strong limestone.

A conveniently simple 'linear' equation, which describes the *non-linear* shear strength behaviour of intact rock over a range of confining pressure from zero (uniaxial), through the brittle-ductile transition, and up to the critical (maximum strength) state was derived by Barton (1976), but appears to have been over-looked up to now. It had the following simplest possible form, and is repeated in Barton (2014):

$$(\sigma_1 - \sigma_3)/\sigma_c = M\,\sigma_3/\sigma_1 + 1.0 \qquad (1)$$

The respective gradients M for Solenhofen limestone (as in Figure 3), Oak Hall limestone, Nahant gabbro and Westerly granite, as tested and reported by Byerlee (1968), showed a logical progression of 3, 7, 9 and 30 as strength increased. Reservoir rocks will clearly be in the lower range of gradients M.

SHEARING ALONG FRACTURES OR JOINTS IS A NON-LINEAR PROCESS

The intended focus of this paper is the potential contribution of rock mechanics understanding to the changing-over-time production from naturally fractured reservoirs. For instance see the emphasis on fracture shearing in Barton (2006, 2007a, 2007b). Shearing during continued production may be *an inevitable condition for continued production*. In addition we will see possible rock mechanics contributions to the ongoing attempt to understand the mechanisms of fracture shear and dilation in stimulated gas-shales. These mechanisms seem to be occurring beyond the central and ellipsoidally-shaped frac-stimulated and propped 'pod' region in tight gas-shales and oil-shales. This is because microseismic activity is detected well outside this 'central' frac-stimulated and propped region. An excellent introduction to this topic was recently presented by Dusseault (2013). The importance of fracture shearing was specifically referred to by Dusseault, although using linear Mohr Coulomb theory.

An extensive review of fracing stimulation methods and results was given by King (2010), but this was with limited emphasis on shearing, more on opening. The very extensive microseismic monitoring results, such as those described by Fisher and Warpinski (2011) nevertheless give clear evidence of the large extent of shearing mechanisms. They *also* emphasized the desireable complexity and fracture-including nature of the fraced region, which needs propping where it is without shearing. Shear and dilation, however slight, needs no propping, if the gas-shale is sufficiently brittle, with high enough static deformation modulus and high enough JCS (joint wall compression strength, from Schmidt hammer '*r* ' rebound).

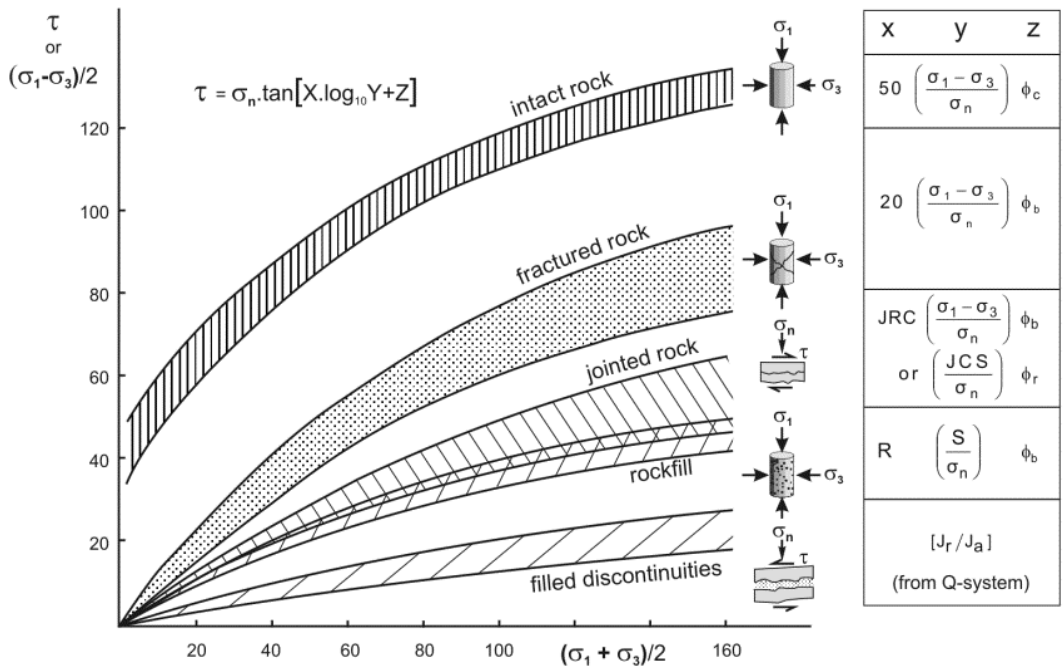

Figure 4 Comparative shear strength trends for at least four of the components of the shear strength of a rock mass (or fractured reservoir). Only the intact rock (and therefore parts of a rock mass) have tensile and cohesive strength. The two first empirical strength criteria fitted high-pressure test data from Byerlee (1968) and Mogi (1966). The third set of empirical x, y and z parameters are for rock joints with variable joint- or fracture-roughness (JRC) and apply to high pressure (reservoir-depth) or lower pressure civil engineering depths

respectively. The joint wall compressive strength (JCS) which can be recorded by Schmidt hammer, is replaced by the triaxially confined strength ($\sigma_1 - \sigma_3$) when considering reservoir depths. Filled discontinuities, of relevance to fault zone conditions have much lower shear strengths, and these can be estimated from the Q-system of Barton et al. (1974) which was summarized in Barton (2007c). See latest presentation of the frictional strength Jr/Ja of the discontinuities such as found in fault zones, in Barton (2013c). (Note that Jr the joint roughness is a rating varying from 0.5 (slickensided/polished) through 1.5 (rough-planar) to 4 (discontinuous). The joint alteration or filling rating Ja varies from 0.75 (healed) through 2 (weathered) to 20 (thickly filled-discontinuity with swelling clay like montmorillonite).

Figure 4 emphasizes the non-linear shear strength of all the strength components of a fractured or jointed rock mass. These strength envelopes are clearly different, due to the non-linearity, to that assumed in most petroleum geomechanics presentations. Only the intact rock, which would represent the 'intact bridges' between the natural fractures, has true cohesive and of course tensile strength. The various empirically-derived (*a posteriori,* not *a priori)* non-linear strength criteria have the general parametric X, Y, Z form illustrated, and in a subsequent figure, the *simple index tests* needed to derive these fracture or rock-joint parameters (wall roughness JRC, wall strength JCS and residual friction φ_r) are each illustrated.

The ratio Jr/Ja described in the caption of Figure 4, is usually close to the friction coefficient μ. Even this simple method is much more accurate than the standard 'μ = 0.85'. The criterion involving JRC, JCS (or σ_1-σ_3) and φ_r is of course the most accurate. It is remarkable that this is not used in the geomechanics usually practiced in the petroleum industry. The parameters are obtained with ease, or can be visually estimated when one is experienced in their use.

The last two parameters Jr/Ja shown in Figure 4 (which have some similarity to JRC/JCS) are used, together with four other parameters, to describe the quality Q of a rock mass in the world of tunneling (Barton et al., 1974). In fact the Q-value, which is derived from block-size and inter-block frictional strength plus an active stress term, is also simply linked to the stress-dependent static deformation moduli E_{mass} and to P-wave velocities (Barton, 2002, 2007c). Permeability can also be estimated. These potentially useful and simple economic methods (it is therefore they are used in tunneling) seem to be unknown in petroleum geomechanics.

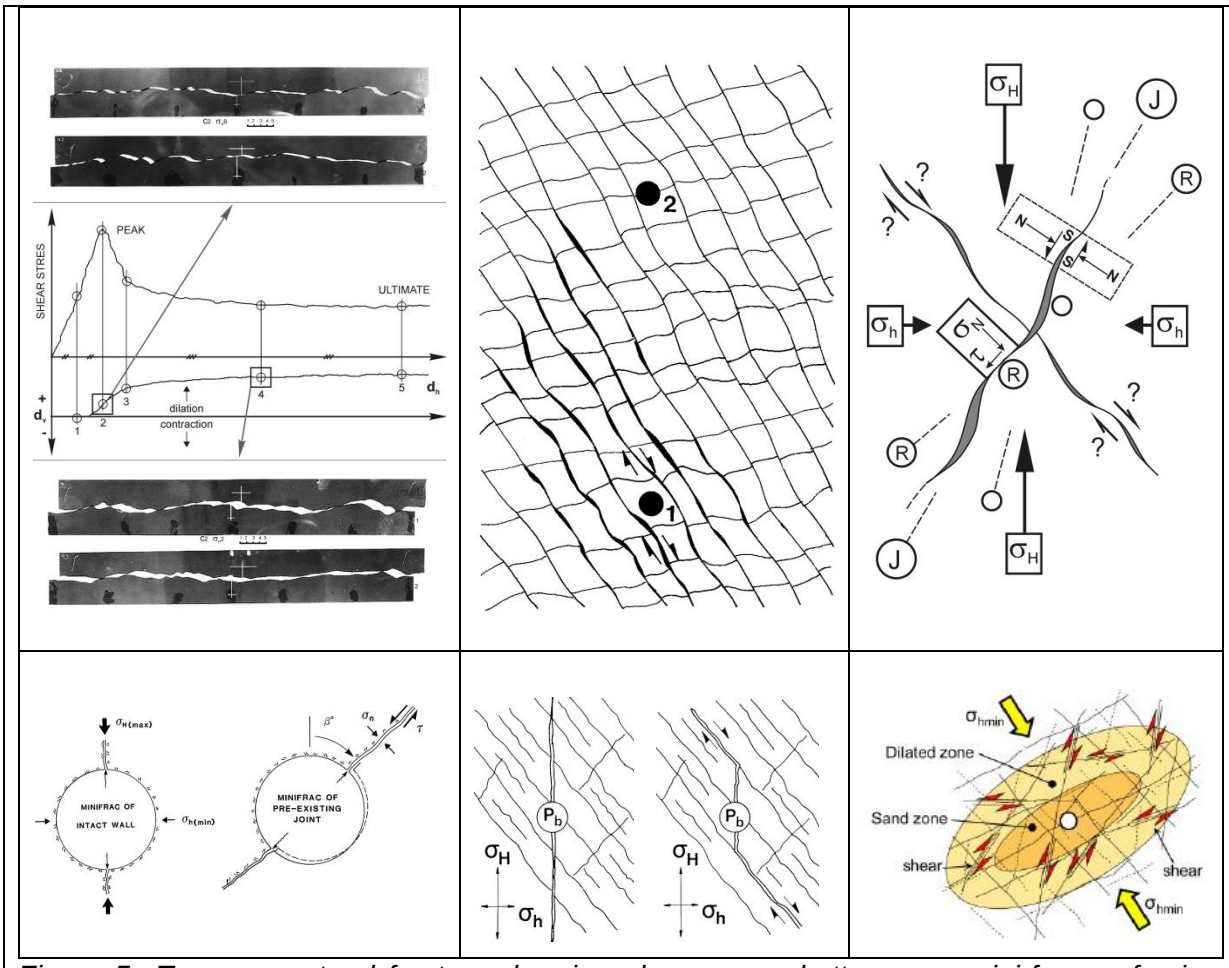

Figure 5 Top-row: natural fracture-shearing phenomena, bottom-row: mini-frac or fracing-induced fracture-shearing phenomena. The top-left figure shows reconstructed fracture shearing events, with correctly measured dilation paths, from Barton (1973). The figure was derived from roughness profiles measured by means of photogrammetry of the surface of weak physical model tension fractures in 1967. These represented 10 m long rock fractures at prototype scale. Note the obvious potential for permeability enhancement with shear, which will be modified by high effective normal stress and possible gouge production due to failed asperities (Olsson and Barton, 2001). The top-centre figure represents the often experienced 'fluid-capture-and-shear' in a geothermal reservoir, as described by Barton (1986). The top-right figure shows conjugate but 'anisotropically-rotated' shearing of a dominant joint or fracture set, and was used by Barton (2006) to demonstrate the potential deviation of polarized shear-wave fast axes from the traditionally assumed geophysicist's 'parallel-to-sigma maximum' direction. Note the fluid-filled 'open' (O) areas due to dilation, and the rock-to-rock (R) contacting and stress-transferring areas. The relative rotation between R and O (exaggerated for illustration) might explain some of the above referred rotation of shear waves. The bottom-left figures show mini-fracing of an intact borehole wall and shearing of a jointed borehole wall, perhaps needing slower pressurization, from Barton (1981).The bottom-centre figures show the assumed effect of fast and slower pressurization in an obliquely jointed rock mass, from Barton (1986). The bottom-right figure is from a Dusseault (2013) keynote lecture, and represents the potential shear-mobilization of fractures in gas-shales, as a result of stimulation by a series of propped hydraulic fractures developed from horizontal wells. Fracture sets are shown oriented in a conjugate pattern in relation to the average parallel-to-sigma-max fracing direction. The resulting microseismic activity 'distant' from the ellipsoidally propped region may be the key to explaining the shearing, slight dilation (if nearly planar fractures) and drainage potential of gas- shales.

Figure 5 is a collection of drawings of fracture shearing spanning the period 1973 to 2013. The mobilization of peak shear strength or the reduction towards residual or ultimate strength is of course of fundamental importance in many of the earth sciences. Joint- or fracture-shearing and the accompanying dilation and permeability enhancement, which are illustrated directly or implicitly in the top three diagrams, affect geothermal reservoir behaviour because today's fracture trends may no longer be parallel to principal stress directions, so the injected cold water may be 'captured' by joint- or fracture-shearing (Barton, 1986) as has occurred in numerous cases. This was also discussed and modelled by Murphy and Fehler (1986) concerning Fenton Hill. The experiences of microseismic due to shearing given by Pine and Bachelor [1984] in the Cornwall HDR (hot dry rock) are well known.

Production from domal reservoirs with conjugate fracturing, and the apparent result of fracing in gas-shales also involve joint- or fracture-shearing. The former is demonstrated later in this paper, from discrete-element (jointed) modelling of compaction in the Ekofisk reservoir. The central hydraulic fractures in frac-stimulated gas-shales branch out in a complicated way (e.g. Fisher and Warpinski, 2011) and apparently cause associated shearing well outside the ellipsoidal propped region, judging by the swarms of microseismic. This is a wonderful contribution to the fracture area in contact with the gas-bearing matrix, in a medium with remarkably low permeability until it is shear-stimulated, some distance from the (mostly) tensile fractured propped-zone.

The shear strength description methods to be described in this paper have been used in rock mechanics and mining for the last 35 years, but seem not to have found their way into petroleum geomechanics, unless the flurry of some thousands of citations to the writer's articles on shear strength in the last four to five years has anything to do with the focus on gas-shales, now in many countries. Regrettably, petroleum companies are often rather 'silent' at workshops, and their levels of application of cross-discipline methods to fractured reservoirs are sometimes hard to judge, as they mostly do not reveal possible advances in front of 'competitors'. This was demonstrated in the Muscat workshop.

FRACTURE CHARACTERIZATION AS PRACTICED IN ROCK MECHANICS

Rock mechanics appears to be very different from the *geomechanics* and *geoscience* practiced by oil companies, their consultants, and by service companies. There is naturally much more focus on the deformability and strength of rock joints or rock fractures in rock mechanics, as this often determines the stability or otherwise, of potentially unstable opencast mine slopes, road cuttings, dam abutments, rock-wedges in rock caverns, etc. The ability to model these discontinuous processes, also with coupling to conductivity and pore pressure, has been provided by distinct element (jointed) models such as Cundall's 2D UDEC (universal distinct element code) and by his 3D 3DEC, each marketed by Itasca. These codes have been available for several decades.

An essential step in this deformation-modelling process is the collection of input data for the constitutive joint- or fracture behaviour modelling. The most widely used *non-linear* method, is the Barton-Bandis criterion described in Barton et al. (1985), which has been a part of UDEC-BB since 1985, and has been incorporated in 'competing' computer codes more recently. The necessary but rapidly and cheaply obtained input data is illustrated in Figures 6, 7 and 8.

Here the widely used terms JRC and JCS are graphically explained by means diagrams and photographs of the simple index tests, and by roughness profiles (giving the scale-dependent JRC) at different block-size length scales of 100mm and > 1m length. (See table of definitions on page 1). JRC applies to block size and not to joint length: in other words it applies to the spacing of cross-joints (in petroleum terminology the spacing of fractures crossing the fracture being characterized). The above is because physical and numerical models involving thousands of blocks indicate that the block dimension is more relevant than the joint or fracture length – which of course could be tens of meters. The block-size scaling of JRC and JCS was first given by Bandis et al. (1981), Barton et al., (1985) and in a series of publications stretching through to Barton (2014). The criterion is widely used in rock mechanics, especially for rock slope stability estimation and design, and for input into numerical models for tunnel, cavern, and dam abutment and dam-loading stability calculations.

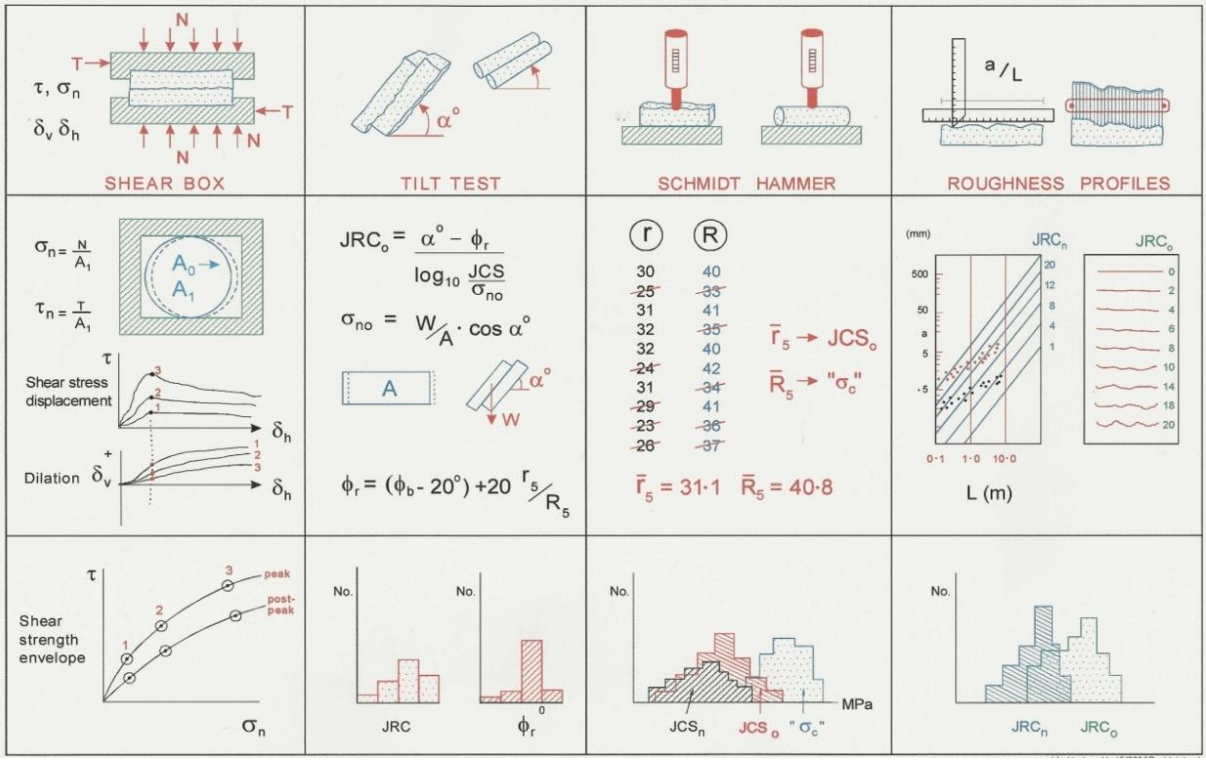

Figure 6 A collection of simple index tests for obtaining input data for fractures or joints, using tests on core or on samples sawn or drilled from outcrops. In the left-hand column, direct shear tests are also illustrated, which can be used to verify the results from empirically-applied index tests. Note that the Schmidt hammer should be used on clamped pieces of core to estimate the uniaxial compression strength UCS or σ_c. This is done on dry pieces of core (rebound R, use top 50% of results). For the joint wall strength JCS, this is done on saturated samples (rebound r, use top 50% of results). These samples also need to be clamped (e.g. to a heavy metal base).Three methods of joint-wall or fracture-wall roughness (JRC) can be used: tilt tests to measure tilt angle α (Figure 7), or a/L (amplitude/length) measurement, or roughness profile matching: the latter obviously more subjective. A standard set of small-scale (length L_0 = 100 mm) roughness profiles, and profiles of >1m (length L_n), with consequently reduced JRC_n values, are shown in Figure 8, from Bakhtar and Barton (1984) and Barton (1999).

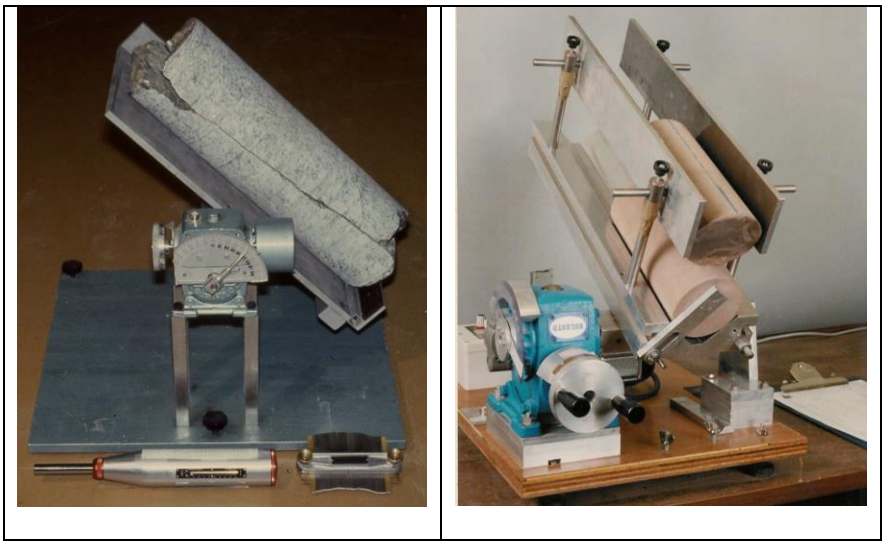

Figure 7 Left: Tilt tests using slow manual rotation of a 1:200 reduction gear. The joints or fractures can be obtained from drill-core or from sawn blocks extracted from a fracture pavement or from a relevant cliff with jointed/fractured analogue-reservoir-rock exposed. The gravity normal and shear loading acting in the tilt tests brings the joint or fracture to shear failure (angle α°, typically 40° to 80° depending on roughness JRC), and this very low stress test (σ_n = 0.001-0.002 MPa) is used to back-calculating JRC. One should use saturated joint/fracture surfaces, but not sufficiently wet to cause suction during the slow rotation/tilt testing. Using the Barton (1973) and Barton and Choubey (1977) non-linear peak strength criterion (see equations 2 and 3), shear strength (and shear stiffness) can be estimated at three to four orders of magnitude higher stress, relevant to reservoir depths. In the left-hand photo a Schmidt hammer and a roughness-profiling brush-gauge can also be seen.

Right: Tilt tests on (dry) core sticks for measuring the basic friction angle φ_b of unweathered surfaces of the reservoir rock (typically shear failure / sliding at 28° to 32°). The core sticks should be smooth-flat (not polished, nor with ridges). Final preparation can be with sand-blasting. These tests have been used in rock mechanics since their development in Barton and Choubey, 1977. They were used in 1985 and 1986, perhaps for the first time in a reservoir context, in Ekofisk reservoir compaction studies, for characterizing the conjugate joints in the porous chalk. Barton et al. (1986, 1988), Barton (2013a).

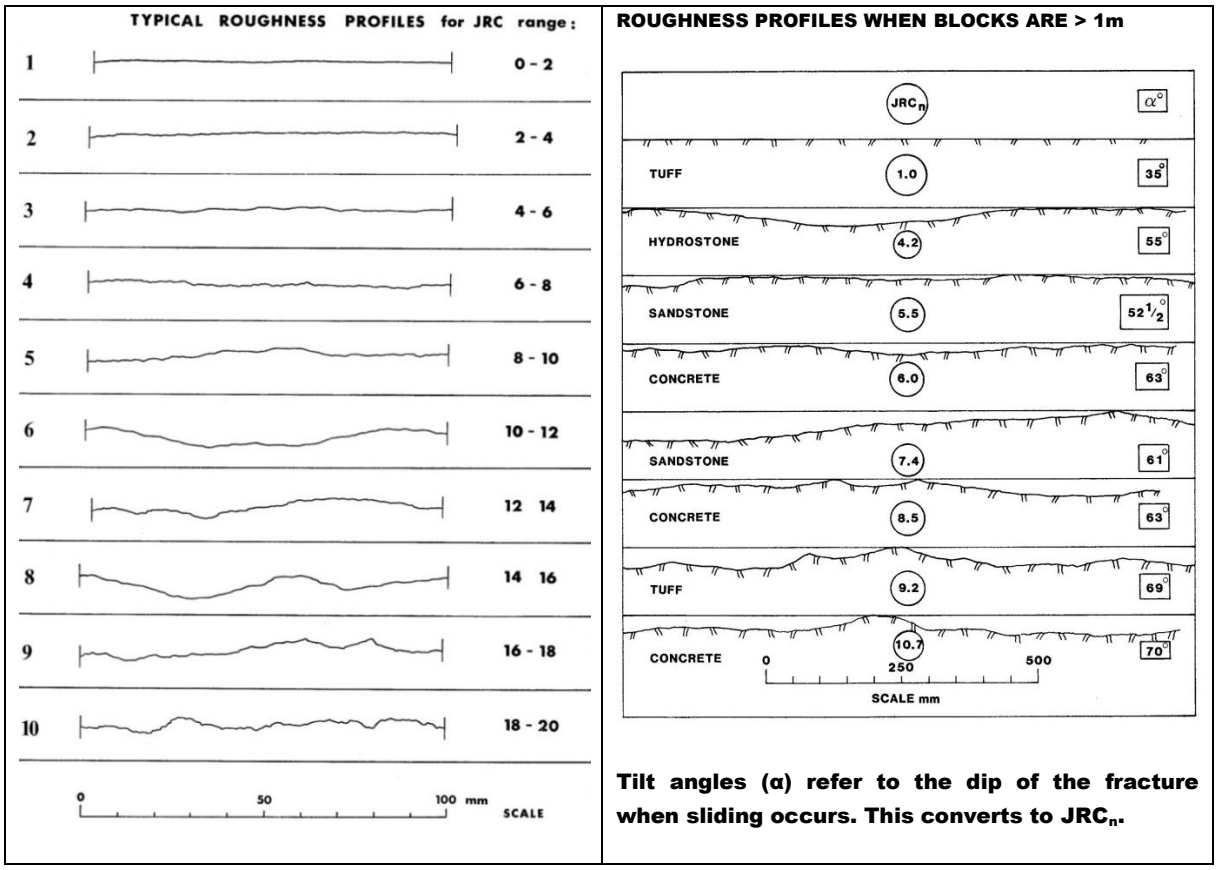

Figure 8 Left: A simple scheme for approximately characterizing the small-scale roughness (JRC_0) of joints or natural fractures, from Barton and Choubey (1977). Right: Large-scale roughness profiles (showing JRC_n), from Bakhtar and Barton (1984). The source of these longer profiles was diagonally-fractured ≈ 1 m^3 blocks, with fracture formation controlled by a flat-jack applied principal stress parallel to the tensile-wedging direction. Some photographs of these 30 years-old samples are given in Barton, 2014. A combination of these roughness scales could be used when logging fractured pavements, and indeed could be applied to the analysis of high quality 'drone' photos. The preferred way is nevertheless to perform amplitude/length (a/L) profiling as illustrated in the top right-hand side of Figure 6, or to perform tilt tests on joints or fractures in recovered drill-core, as illustrated in Figure 7.

JOINT OR FRACTURE SHEAR STRENGTH AND COUPLED 4D MECHANISMS

The tilt tests illustrated in Figures 6 and 7 are used to back-calculate the roughness coefficients JRC illustrated in Figure 8, using the Barton (1973, unweathered) or Barton and Choubey (1977 weathered) non-linear peak shear strength criteria. These were developed in order to provide more accurate values of shear strength than the standard linear Mohr-Coulomb approximation. When in situ size blocks are involved, the block-size scaled *Barton and Bandis* shear strength criterion (Bandis et al. 1981) is used, with the subscripted parameters JRC_n and JCS_n signifying in situ (reservoir-estimated, pavement-estimated, or cliff-estimated) block sizes of nominal side-length L_n as compared to the nominal laboratory (core-sample) sizes of L_0.

The three non-linear equations are listed below. They are direct decendents of two hundred direct shear tests on rough tension fractures developed in brittle model materials (e.g. Figure 5, top-left), in which 'roughness' was 20, wall-strength was UCS (since no weathering) and the basic friction angle was 30° (also because of no weathering).

$\tau = \sigma_n' \tan [JRC \log_{10}(JCS/ \sigma_n') + \varphi_b]$ (Barton, 1973) (2)

$\tau = \sigma_n' \tan [JRC \log_{10}(JCS/ \sigma_n') + \varphi_r]$ (Barton and Choubey, 1977) (3)

$\tau = \sigma_n' \tan [JRC_n \log_{10}(JCS_n / \sigma_n') + \varphi_r]$ (Bandis et al., 1981) (4)

Note that the 'complicated non-linear term' involving $\log_{10}$ provides both the *peak dilation angle* and the *asperity failure* component S_A which can be of almost equal (angular) magnitude. When generating shear-displacement-dilation-permeability coupling behaviour, the concept '$JRC_{mobilized}$' from Barton (1982, 1986) is used. Some simple hand-calculated examples are given later in this paper. These methods may be the key to a quantitative understanding of gas-shale stimulation results. Of course they are also fundamental for production from 'critically stressed' NFR. We can move far beyond 'μ = 0.6, 0.85, 1.0' by using simple non-linear rock mechanics.

The above fracture roughness and strength parameters JRC, JCS and φ_r allow one to generate the desirable *shear-dilation-permeability* enhancement curves, as probably operating in stimulated gas-shales, and the much less desirable *stress-closure-permeability* reduction behaviour that makes itself known in stress-sensitive reservoirs, or later on in the life of a producing reservoir. Each of the above occur in the context of potential reservoir 4D behaviour – which is far more interesting and sophisticated than 'stress and strain', an over-simplification suggested by authors working in a major service company. This type of non-linear, rock mechanics based 4D coupled behaviour modelling seems to be rare or absent in petroleum geomechanics. Great sophistication is seen in many other areas but maybe not this one. (If it is in fact occurring but is not published due to confidentiality rules, then the present article could perhaps be considered a contribution to the 'open literature').

Experimentally measured examples of joint or fracture-closure and shear are illustrated in the top of Figure 9. The top two diagrams illustrate measurements (from Bandis et al., 1981, 1983), of normal stress-closure, and shear-displacement tendencies for jointed blocks of different sizes. Note the scale effect, which is most prominent when joints or fractures are rough. In the central diagram, use of these deformation components was applied by Barton (1986) in order to predict the relative strengths of the normal-closure component, which was termed N, and the shear component which was termed S.

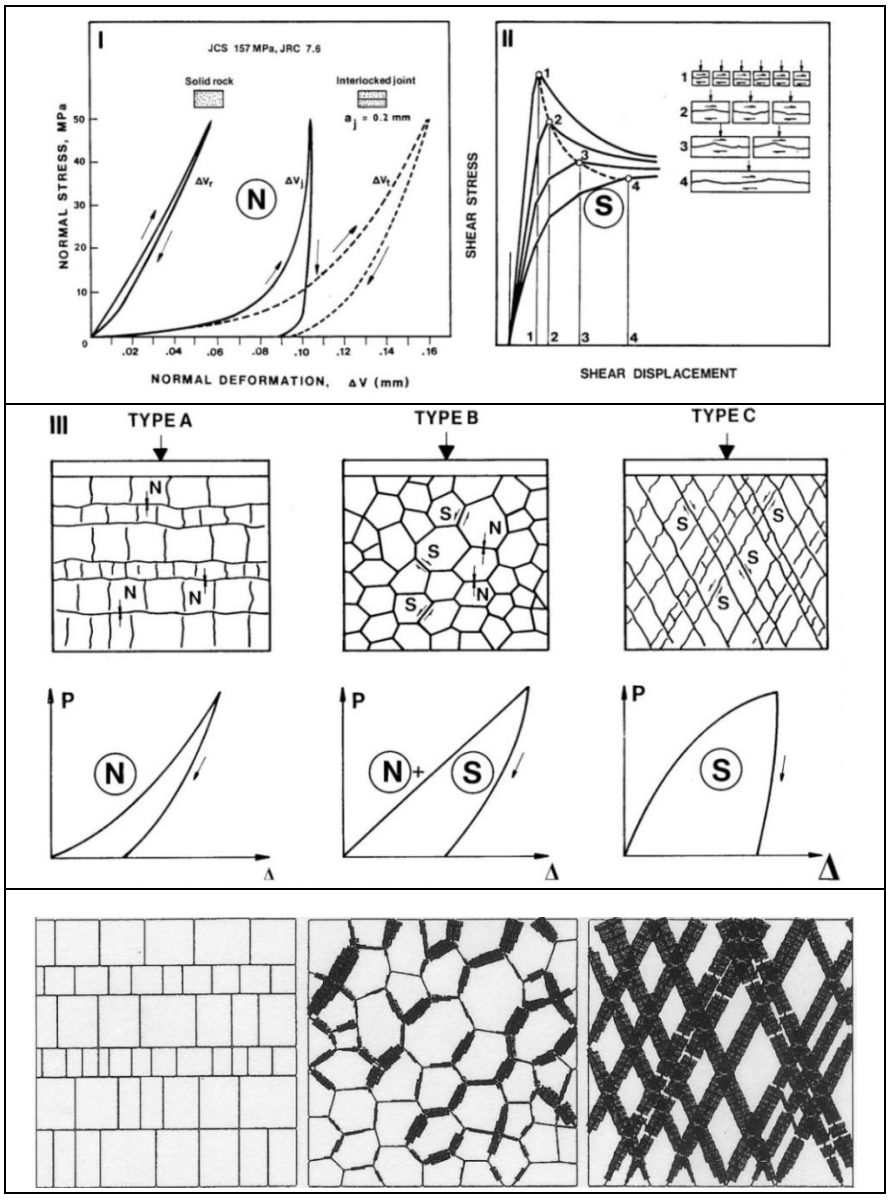

Figure 9 The non-linear normal-closure (component N) and non-linear shear-deformation (component S) combine to form distinctive behaviour in the fractured rock mass, with conjugate shearing giving the most impressive potential contribution to NFR and fraced gas-shale productivity. From Bandis et al.(1981, 1983), Barton (1986) and Chryssanthakis et al. (1991).The shear displacements along the modelled rock joints were modelled by UDEC-BB. Use of this code requires input for JRC_0, JCS_0, φ_r and relative block-size L_n for the different joint or fracture sets in relation to the test dimension L_0. The internal workings of the code automatically provide block-size and stress-dependent shear strength, shear stiffness, normal stiffness, and the coupling of physical aperture (E) and hydraulic aperture (e) where the intrinsic joint or fracture conductivity $k = e^2/12$. Note that P and Δ are the applied axial load and resulting axial deformation. When loading biaxially and recording lateral expansion as well, a strong 'Poisson ratio' or lateral expansion may be experienced, which in the case of Type C (conjugate shear) will far exceed the elastic limit (0.5) and even exceed 1.0 due to the combined effects of shearing and dilation.

The three basic rock mass load-deformation processes illustrated in the middle of Figure 9 are respectively concave, 'linear' and convex. The linearity is due to a 'cancelling-out' of the two opposing non-linear tendencies. Each of these three modes of behaviour have been confirmed by large-scale *in situ* testing, including flat-jack loading of an $18m^3$ (2 x 2 x 4.5m) block sawn into columnar basalt at the Hanford-Washington site, one of many studies related to possible high-level nuclear waste disposal in the 1980's.

The UDEC-BB models shown at the bottom of Figure 9 were performed several years later, and help to reinforce the idea of a potentially positive contribution of conjugate shearing to maintenance of productivity. However this process, which was also illustrated in Figure 5, requires some shrinkage of the matrix to 'make space' for the shearing, if one-dimensional compaction is the average boundary condition, such as in the case of a compacting reservoir. Porous deformable chalk and weaker limestones would be suitable candidates.

Coupled shear flow tests (CSFT) performed by Makurat on Ekofisk chalk using either equilibrated sea water or Ekofisk oil, confirmed the maintenance of permeability due to shear, even under high effective stress levels. Some of the associated testing and modelling performed at NGI for the NPD (Norwegian Petroleum Directorate) was described in Barton et al. (1986, 1988). The CSFT method was described in detail in Makurat et al. (1990). Such coupled-process tests seem to be quite rare in the petroleum industry, although there are some notable Ph.D studies of shear-flow coupling in recent years potentially related with nuclear waste disposal scenarios.

A decade after these Norwegian coupled shear-flow studies for Ekofisk, the Stanford University group of Zoback and co-workers found convincing evidence of the importance of (interpreted) shear stress on whether fractures in *crystalline rocks* were conducting or not conducting, based on deep well-log analysis. The work of C.Barton et al. (1995) and Zoback and Townend (2001) is important confirmatory evidence of the conductivity-related value of shear stress. Joint- or fracture-shearing seems to be an essential component of successful gas-shale stimulation, but can be problematic for geothermal reservoir operation, as it was in the case of the Cornwall 'hot dry rock' project, if 'fluid-capture-due-to-shear' occurs, as sketched in Figure 5.

The importance of shear stiffness and associated block-size scale effects

Figure 10, from Barton (1982), demonstrates something which has potential application to understanding the process of gas-shale stimulation: namely the quite low shear stiffness which is also related with block size. To be strictly correct this should be termed the *peak shear stiffness*, which is shown defined in Figure 10, left-inset.

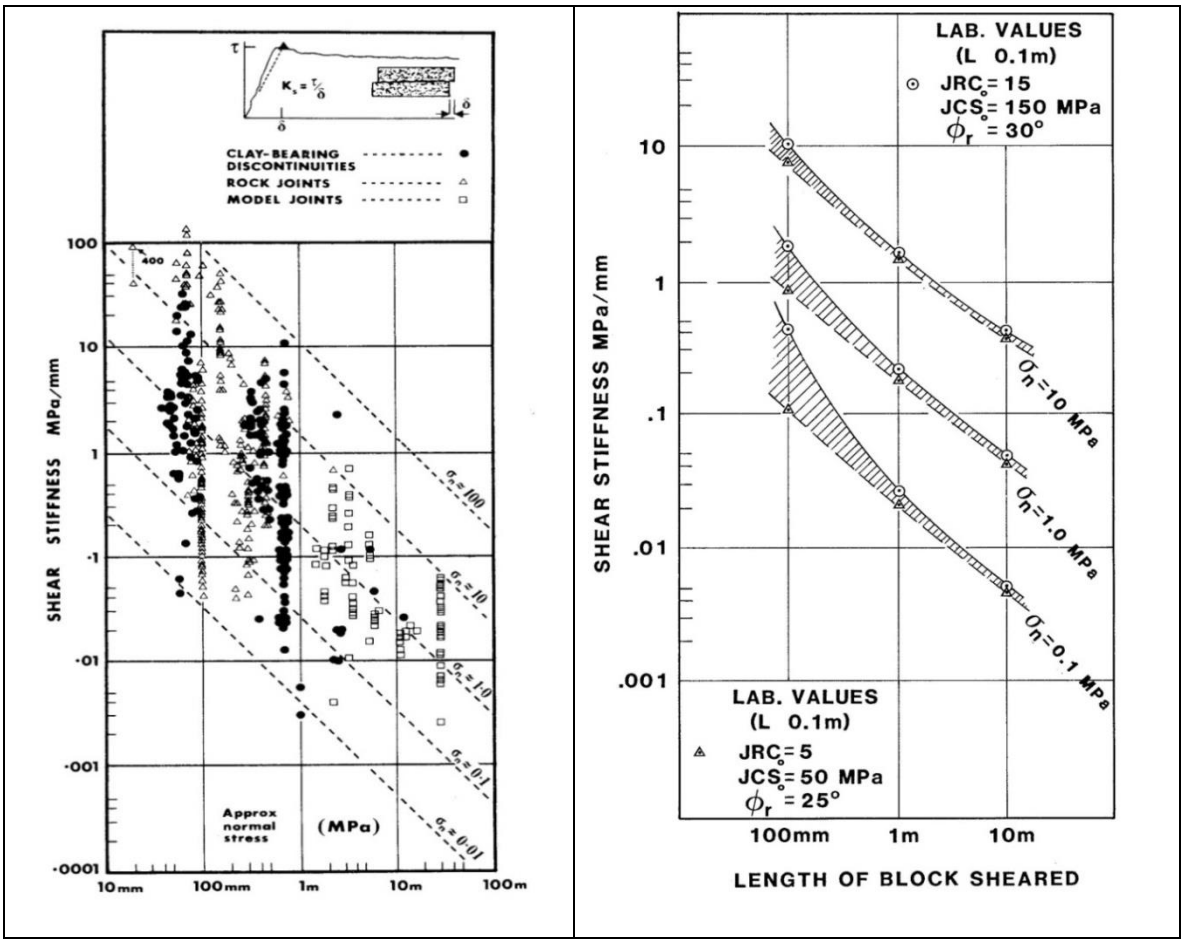

Figure 10 The inset (left) shows how shear stiffness (Ks) is estimated. This important parameter is strongly affected by all three 'joint parameters' (JRC, JCS and φ_r), and is doubly (block-size) scale-dependent, due to peak strength and displacement-to-peak scale dependency, as described in Barton (1982) and Barton et al. (1985). The parameter Ks is probably fundamental to oil shale and gas-shale stimulation success or failure.

Both diagrams in Figure 10 show the effect of block size and normal stress on the resulting peak shear stiffness. The diagram on the left shows experimental data assembled by Barton (1982). As detailed in the figure caption, there is a beneficial double scale effect, meaning that *in situ* (larger blocks) (of e.g. gas-shale) will have significantly lower stiffness than laboratory (core-size) samples. The diagram on the right shows calculated peak shear stiffnesses for two different sets of input data. The lower example has JRC_n , JCS_n and φ_r values that are more in line with gas-shales, but likely to be on the high side.

Shear stiffness in situ is significantly lower than generally listed in software company instruction 'manuals' as the double scale effect seems not to be widely appreciated, and shear stiffness is seldom or never mentioned when assessing the likely mobilization of friction in 'critically stressed' reservoirs. The reality is that friction starts to be mobilized at small strain, followed by the gradual mobilization of roughness towards peak shear strength. The use of $JRC_{n\ (mobilized)}$ and other parameters that are

also variables, gives greater understanding than using simple friction coefficient mobilization, which refers only to a single (peak) resistance. The key question is what level of effective normal stress is likely to be operating in a frac-stimulated gas-shale in the 'surrounding' volume, where fracture shearing is occurring? In addition, what is the typical block size for scaling purposes?

As an 'anchor' for such deliberations we may refer to the four photographs of interbedded shales and siltstones, from the unique North Sea source-rock location in Dorset in Southern England: at Kimmeridge Bay. Here we can imaging the branching that is likely to occur when frac-stimulating gas-shale, as for instance described by Fisher and Warpinski (2011) and King (2010).

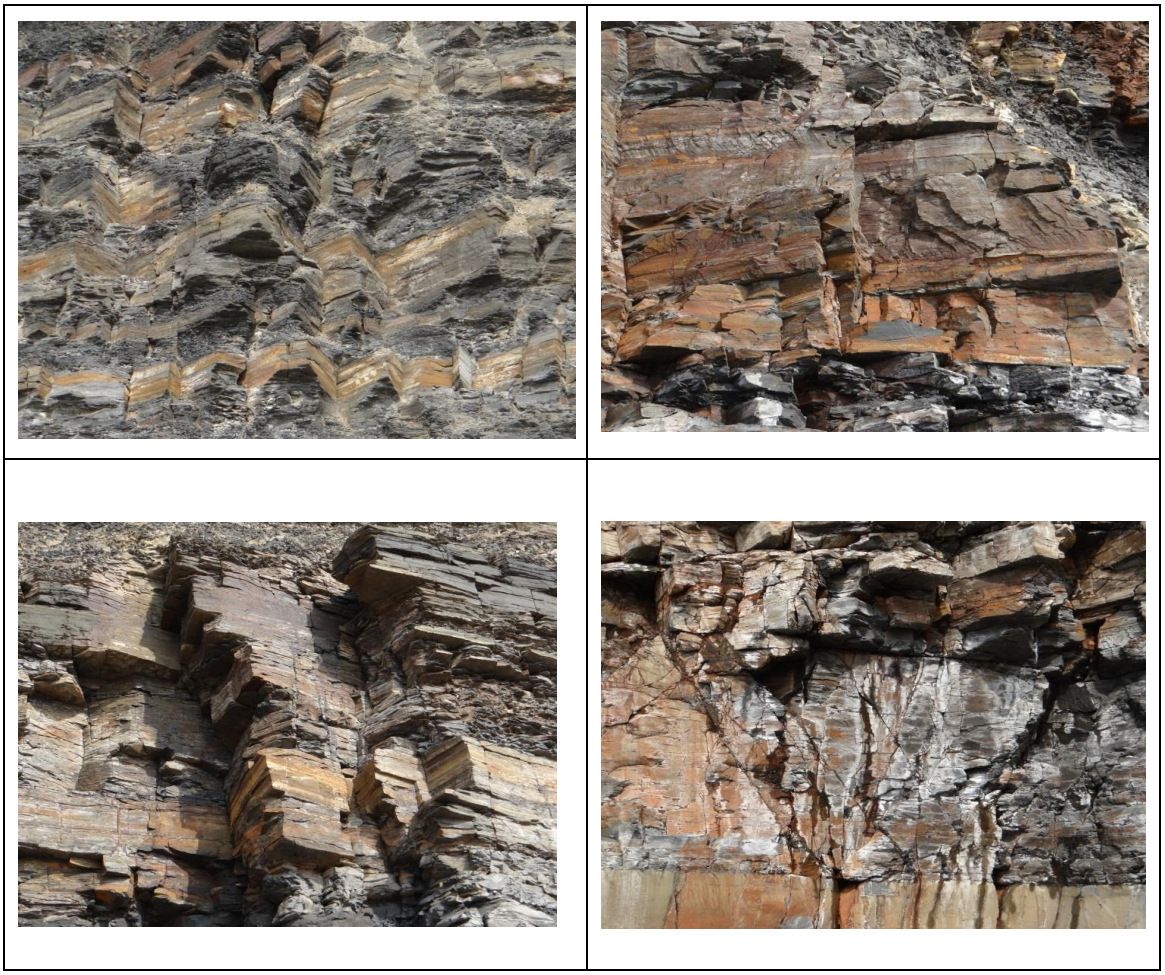

Figure 11 Examples of quite planar bedding, and quite planar vertical joint sets with low Jr (1.0-1.5) and low JRC_n (maybe 1 to 3). Also exhibited is steeply dipping jointing. These shales with inter-beds of siltstone and occasional dolomite, are from the source-rock location Kimmeridge Bay in Dorset, S. England. It is fairly easy to visualize that a lot of branching of hydraulically driven and e.g. sand-propped fracs would occur in such a medium, with plenty of opportunities for fracture shearing, the latter due to relatively low shear stiffnesses. Shear stiffness $Ks = \tau_{peak} / \delta_{peak}$ will tend to be quite 'low' in gas-shales if the relative planarity of the joints (low JRC_o and lower still JRC_n) seen here, is in any way typical.

The examples of interbedded shales and siltstones in Figure 11 may have some possible relevance to the appearance of gas-shales in general because in the words of a gas-shale fracing reviewer like King (2010): ‘no two shales are alike’. This appears to be an important message, and may result in changes to the stimulation techniques, due to shale fabric and stiffness changes, resulting in local rock stress changes. The word ‘shales’ is used mostly as a particle-size indicator. The shales may also be very fine-grained siltstones as indeed suspected in various locations around Kimmeridge Bay.

EXAMPLES OF APPLICATION OF JRC AND JCS

Brief examples of the application of JRC and JCS in petroleum engineering and in tunnelling are finally shown in order to demonstrate some additional features of non-linear coupled BB (UDEC-BB) modelling of rock mechanics (and potential reservoir) processes. Figure 12 illustrates one-dimensional compaction modelling of a representative 1 x 1 m ‘window’ of porous-and-jointed parts of the 14 x 9 x 0.3 km Ekofisk reservoir in the North Sea. An assumed 20 MPa reduction in oil pressure causes sufficient effective stress increase to cause compaction of the non-linear matrix, such that space is made for (anisotropic) joint shearing (shown by ‘flags’), despite the one-dimensional restraint on compaction.

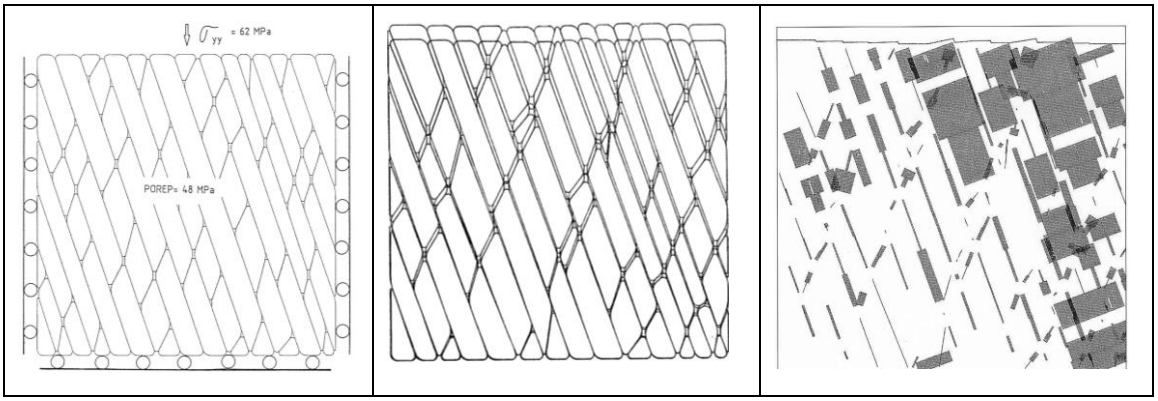

Figure 12 Application of coupled-modelling simulation of reservoir compaction, performed by Christianson, following Itasca/NGI integration of the BB model in the distinct element code UDEC in the new form UDEC-BB in 1985. This discrete element (jointed) model of a ‘1 m window’ in the Ekofisk chalk, was loaded by reducing the pore pressure from 48 to 28 MPa. This caused some shrinkage of the matrix, which made space for joint shearing despite the ID roller-boundary compaction restraint. Jointed/fractured cores of Ekofisk chalk recovered by Phillips were sampled by the author from core stored in Bartlesville, during NGI’s project for the Norwegian Petroleum Directorate. The joint/fracture samples were characterized as illustrated in Figure 6, in order to derive representative values of the three strength parameters JRC_n, JCS_n and φ_r. See Barton et al.(1986 and 1988). Note that the modelled shearing, shown by ‘flag-thickness’ is anisotropic, and clearly not parallel to the vertical applied principal stress. See Barton (2006) concerning the limitations of the ‘parallel-to-major-principal-stress’ shear wave fast axis model, which seems to be much sought after in the geophysics literature. There may in fact be deviation (many cases were documented in Barton, 2006). There has to be deviation of the fast axis, in the anisotropic semi-conjugate case illustrated here, resulting from the domal reservoir.

As a matter of ‘proof of shear’, *slickensided* polished joints were reportedly recognized by Phillips geologists (pers. comm. Helen Farrel), in recovered core from the mid-eighties Ekofisk water-flooding project. Such features *had not been seen* during exploration 15 years before. As also with gas-shale, some shearing is the key to enough dilation and the development and maintenance of some measure of permeability and therefore gas drainage.

The coupling of the desirable *shear-dilation-permeability* and the undesirable *normal closure-permeability*, and the differentiation of hydraulic (e) and physical (E) joint or fracture apertures, as occurring ‘in deep back-ground’ in the above numerical modelling, has been part of rock mechanics modelling since 1985, and it would seem to be applicable in the petroleum industry, if not already used, especially with the recognition of so much ‘remaining’ production (perhaps > 60%) from fractured and unconventional (shale) reservoirs.

Figure 13 is an example of coupled UDEC-BB modelling from a different field than reservoirs. Nevertheless it is a convenient way to demonstrate the depth or stress dependence of the two apertures E (physical: left diagram) and e (theoretical smooth-wall hydraulic: right diagram). Note that shearing-induced dilation or tensile opening can open the physical aperture sufficiently for e and E to be equal. This usually occurs when apertures reach approximately 0.5 to 1.0 mm, as can be seen in Figure 14, for the case of the larger (rougher-walled) JRC_0 values.

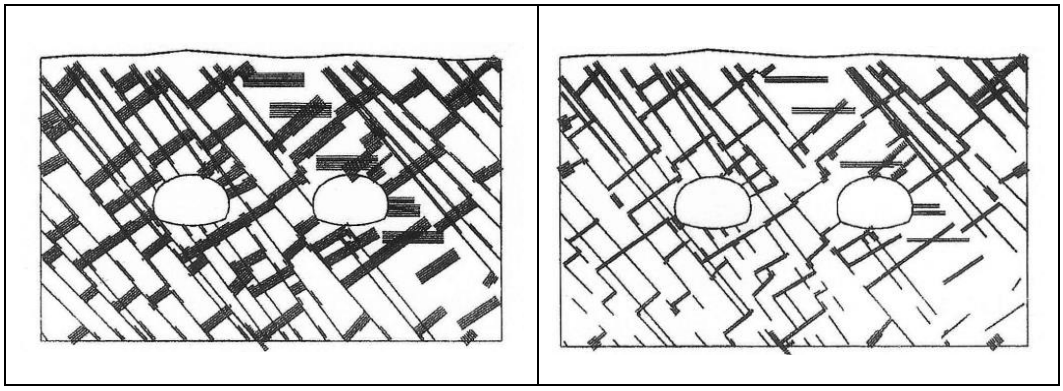

Figure 13 UDEC-BB model of twin tunnels in limestones and shales, from Makurat and Barton (1988). This non-reservoir case is presented here in order to illustrate the two modelled apertures and also to demonstrate that they are both depth or stress dependent. Of course both apertures will be extremely small (a few microns size) at kilometers depth in gas-shales, until shearing and (slight but sufficient) dilation occurs. Fracture aperture E (physical) and e (theoretical) are both tracked in the non-linear Barton-Bandis model, based on the JRC_0 dependent conversion from E to e shown in Figure 14. Permeability, or more correctly joint- or fracture-conductivity is determined by the smaller hydraulic aperture (e) (with $k = e^2/12$), unless the matrix is significantly permeable as well. In the different context of reservoirs, petroleum reserves lie in the matrix pores and in the larger physical joint- or fracture-apertures (E), especially in the case of fractured basement reservoirs in granites, which have high fracture porosity and low matrix porosity. The apertures which can be back-calculated from flow tests or from interpretation of production are the usually much smaller hydraulic apertures (e), so reserves in basement fractured reservoirs need to be greatly upgraded if the E>e mismatch has not been allowed for.

Conversion between physical and hydraulic apertures was a subject that pre-occupied the author a long time ago. In Barton (1972) a graph was shown in which recent tests conducted at the University in Trondheim were interpreted such that the ratio of E/e could be expressed as a function of the hydraulic aperture. Later, in Barton (1982) more data was collected and interpreted showing that the small-scale roughness JRC (strictly JRC_0) had an important role to play in the ratio E/e. This is logical as JRC can be estimated from the ratio of roughness amplitude (a) and length of profile (L), therefore being equivalent to relative roughness in hydraulics, though at much larger scale.

Figure 14 (left) shows the empirical model for converting between e and E in the case of normal closure. Successively more experimental data is given in Barton (1982), Barton et al. (1985) and Barton and Quadros (1997). In the case of shearing with possible gouge production (Figure14 right), the E/e data inclines from left down to the right, crossing the coloured curves on the left. *In situ* block test data had shown this in 1985, and a formal improvement in the model converting E to e and vice versa, was published by Olsson and Barton (2001), following Ph.D. studies of Olsson externally-examined by the writer. The term $JRC_{mobilized}$ was used in the new conversion of e to E for the case of shear. So we have the two forms:

1. For normal closure: $e = E^2/JRC_0^{2.5}$ (5)
2. For shear (and possible gouge) : $e = E^{1/2}\ JRC_{mob}$ (6)

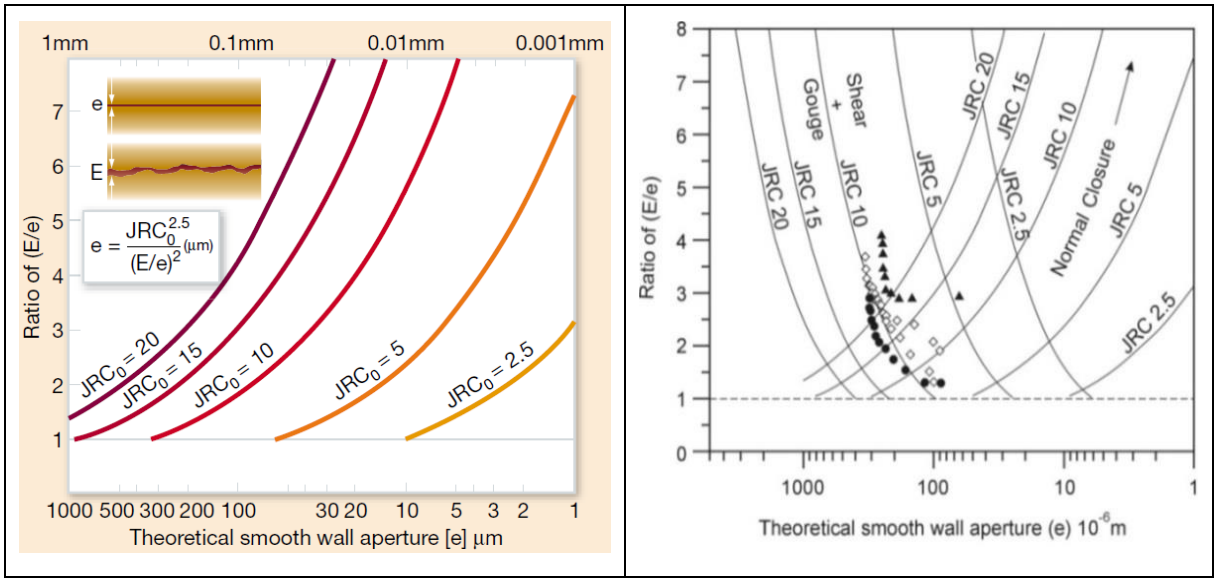

Figure 14 Left: This E/e conversion (from Barton, 1982) applies to normal closure. When shear (and possible gouge production) is involved, a modified form of E/e conversion is used, using the 1982 JRC $_{mobilized}$ concept. This is shown on the right, from Olsson and Barton (2001). In practice the 'JRC-curves' are steeper and incline upwards to the left instead of up to the right as in the original model. JRC $_{mobilized}$ tracks the mobilization of roughness pre-peak and the degradation of roughness post-peak. It is shown in Figure 15. In situ block test data from Barton et al.(1985), and laboratory shear-flow data from Olsson (Olsson and Barton, 2001) gave evidence for the need for this adjustment for shear, with possible permeability losses due to gouge. Note that the permeability eventually increases most in the direction

perpendicular to the shearing direction, as suggested and demonstrated by Gentier (1987) in the late eighties.

COUPLED SHEAR-DISPLACEMENT DEPENDENT BEHAVIOUR

The dimensionless model for $JRC_{mobilized}$ shown in Figure 15 is a useful device for understanding the consequences of shear displacement: namely the mobilization of friction, then mobilization of roughness and eventual degradation of roughness post peak. This empirical model, designed to match measured reality, is of course more sophisticated than just the discussion of 'friction coefficient' (mobilized or available) in so-called critically stressed reservoirs, following the 'Stanford' model, which is seemingly referred to and used by most petroleum companies.

More important than its apparent lack of application outside rock mechanics, is that it provides the ability to generate shear stress-displacement and dilation-displacement, and therefore also permeability-displacement curves for any desired sets of BB input data. The dimensionless model was developed in Barton (1982) as a means of representing shear tests results. Direct shear tests are also apparently rare in petroleum geomechanics. This non-linear part of rock mechanics practice does not appear to be part of the already complicated petroleum geomechanics, although thousands of additional citations to such methods in the last 5 to 6 years perhaps suggests that changes might be occurring.

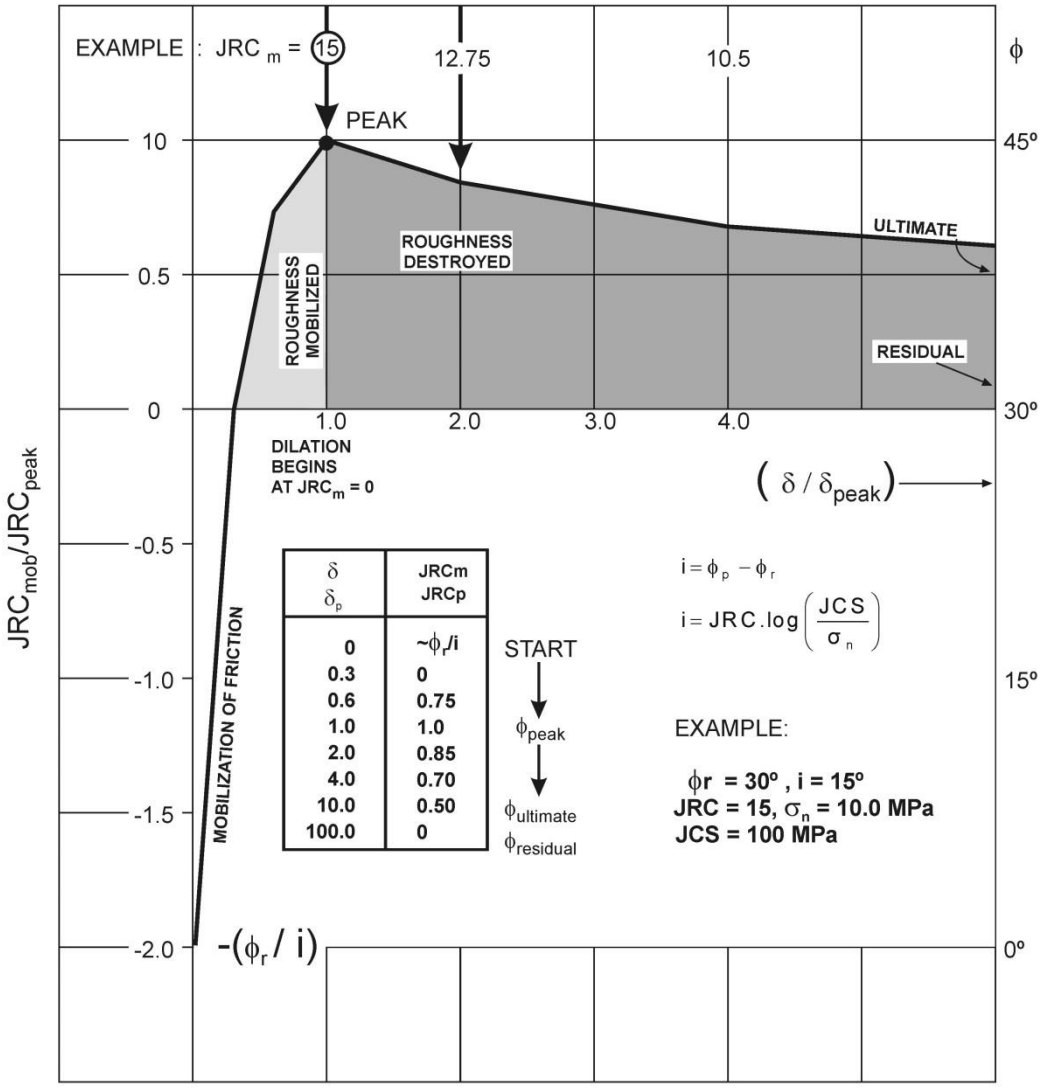

Figure 15 An essential part of coupled process modelling involving joint or fracture shearing is the ability to track shear deformation. The $JRC_{mobilized}$ dimensionless model shown in this figure was developed by Barton (1982). This version is from Barton (2006, Chapter 16 concerning shearing processes in rock mechanics). When one conducts direct shear tests on different joint or fracture samples at widely different normal stress levels, a series of widely differing shear stress-displacement (and dilation-displacement) curves are obtained. The dimensionless quantities (JRC_{mob} / JRC_{peak} and δ/δ_{peak}) represented in the 'universal' diagram shown here, has the effect of consolidating all experimental shear test results into one narrow band with the approximate shape shown here. We can therefore use this single simple device to generate widely different shear stress-displacement and dilation-displacement curves for any desired input data (including variable block size and variable effective normal stress, as shown in Figure 16. The 'look-up' table of values (see inset) is of course smoothed in the UDEC-BB sub-routine.

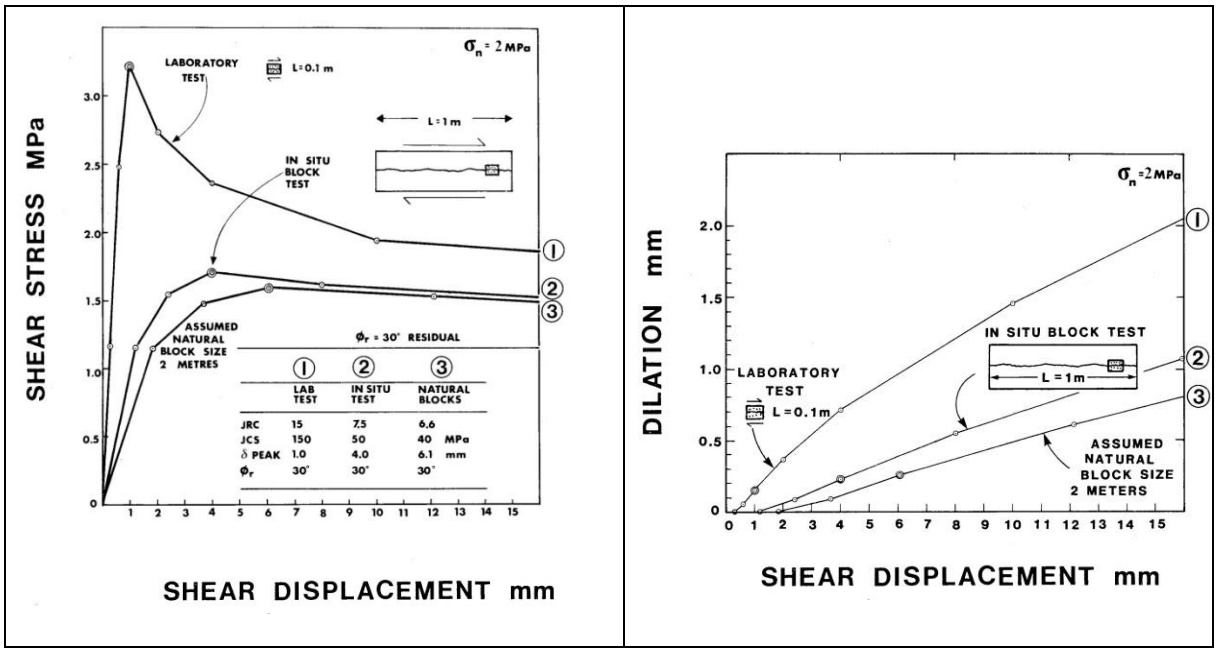

Figure 16 An important and favourable feature of stimulated production of gas-shale is that the shear strength of rock joints or fractures is block-size dependent, as shown in this hand-calculated demonstration from Barton (1982). Shearing may be 'easier' than expected. Note that the space created by shearing-induced dilation will be compromised at high effective normal stress, due to reduced dilation and possible/probable gouge production. It will be noticed that a dilation 'delay' is involved, which may be something to consider when stimulating gas-shales. In other words a significant fracing and propping is needed in the 'central' ellipsoidal volume to push the surrounding shale beyond the 'dilation delay'. The latter will be more marked when block size is larger, as can be seen in the right-hand diagram. However, only a very few millimeters of shear is needed to greatly enhance the potential permeability. Even with gouge production, the coupled shear-flow tests of Olsson showed one and a half orders of magnitude of conductivity increase with only 4 to 5 mm of shear deformation. The models shown in Figure 17 are without any gouge correction, but the E/e conversion already corrects for the tortuosity/out-of-plane effects of rock-to-rock contact across the stressed joints or fractures.

The shear-displacement and dilation-displacement diagrams shown in Figure 16 indicate approximate estimates of the displacement needed to reach peak shear strength (δ_{peak}), which is an important component of the shear stiffness estimate. It is found that peak strength may be reached after a shear displacement of about 1% of the sample length in the case of small (100 mm long) laboratory samples, but this percentage reduces with larger block sizes.

A large body of such data (some 600 direct shear tests on widely different sizes of samples) was collected in Barton (1982). Unfortunately there is a wide scatter in the experimental results, so there will always remain some uncertainty in the shear stiffnesses and in the onset of dilation, and in the position of the maximum dilation angle, which logically occurs simultaneously with peak shear strength. Note from Figure 14, that when apertures reach about 0.5 to 1 mm (due to shear-induced dilation), there will be little difference between e and E. However, in lower modulus

gas-shales, there will likely be an earlier onset of gouge-with-shear production, which is certainly one of the reasons that higher modulus (brittle) shales are favoured (e.g. King, 2010).

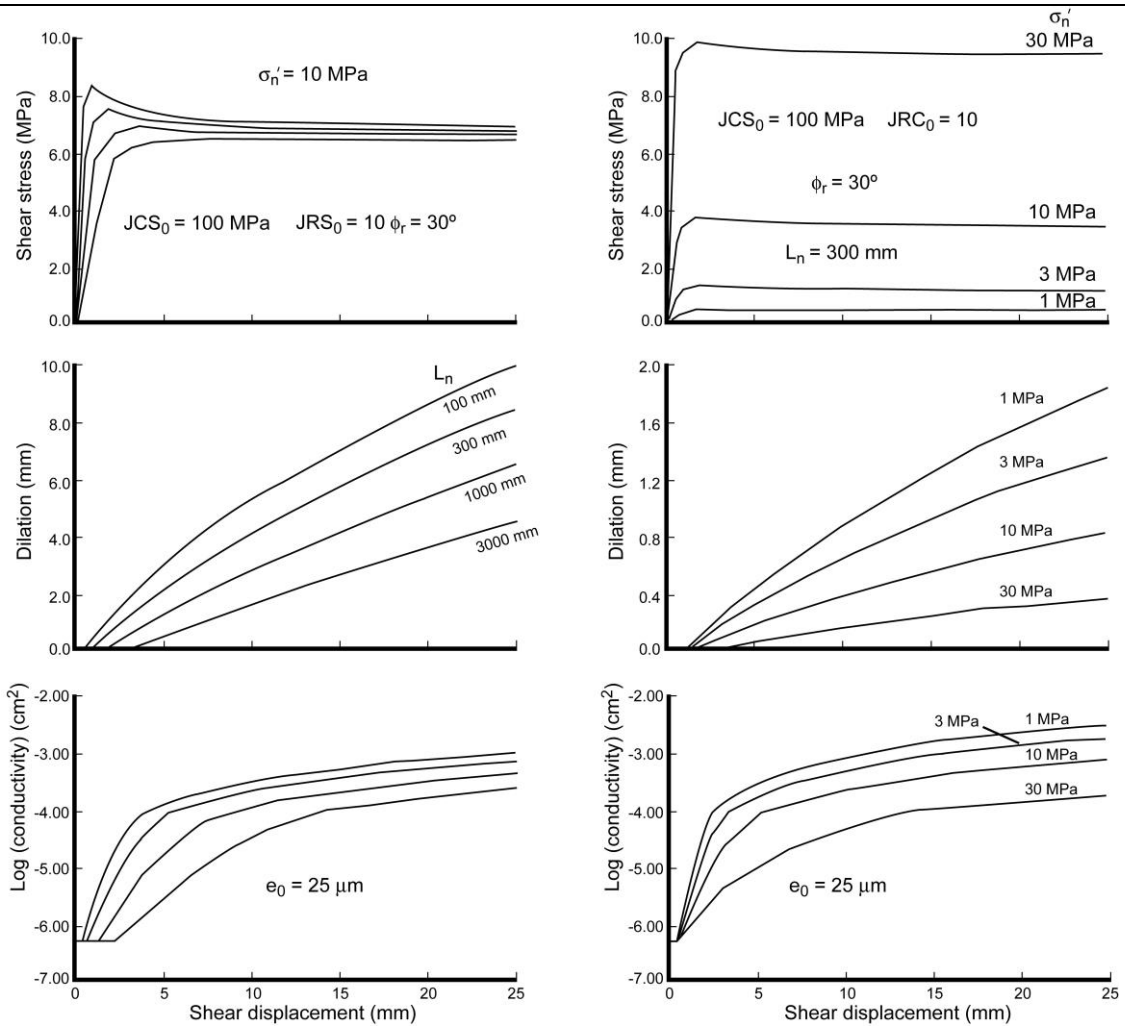

Figure 17 It is appropriate to finish this introduction to non-linear rock mechanics, by assembling an early series of BB coupled-behaviour models generated by Bakhtar on an HP programmable calculator in 1983, while he and the writer were working in TerraTek (now Schlumberger) in Salt Lake City. This was part of a two-volume nuclear waste related study for AECL/CANMET in Canada. These figures were also presented in Barton et al.(1985). The sets of three curves on the left and right are designed to demonstrate the likely effect of block size (on the left), and the effect of effective normal stress at constant 300 mm, a possibly shale-like block size (on the right). Note that the third or lowest set of curves in each case are based on the empirical conversion from physical aperture E to hydraulic aperture e, with an assumed starting point, for these examples, of e_0 = 25 μm. In practice, due to the $JRC_{mobilized}$ mechanism and possible gouge production, the increased conductivity with shear deformation may be less than graphed here, but is likely to remain impressive at least while the shale (or carbonate/chalk) remains brittle or nearly brittle.

The more planar jointing or natural fracturing of gas-shales which can be seen in occasional photographs of exposures of shales in the literature, a planarity also represented in Kimmeridge Bay shales in Figure 11, suggests that a significantly

weaker scale effect will be seen in the case of gas-shales than the ‘strong-scale-effect’ examples represented in Figure 16.

Nevertheless, the assumed peripheral shearing and source of microseismic activity registered in frac-stimulated gas-shales, will be occurring ‘more easily’ than might be suspected if ‘only’ lab-scale coupled shear flow tests (CSFT) have been performed by the industry since the ‘discovery’ of producible/frac-able gas-shales nearly a decade ago.

The same conclusion can be levelled at the 1985 CSFT tests performed on conjugate Ekofisk joints. Production/compaction induced shearing occurs more easily than in laboratory tests because of the larger in situ block sizes. This is why it is useful to have discrete fracture models like UDEC-BB for investigating possible mechanisms at convenient scale (as in Figure 12), before attempting to up-scale the phenomena and represent *likely trends with time* in reservoir models.

As will probably have been understood from this introduction to non-linear (non Mohr-Coulomb) rock mechanics, a strong contribution to an understanding of the effect of time and reduced pressure should be possible, if some of the methods shown are adopted in petroleum geomechanics. The possible need for water flooding earlier rather than later might also be appreciated, after rejecting linear strength envelopes, which cannot apply to the petroleum industry’s usually large changes of effective stress.

CONCLUSIONS

1. Non-linear shear strength, as opposed to inaccurate Mohr-Coulomb linearity, plus nearly critical-state (horizontal strength envelope) conditions may be experienced by weaker reservoir rocks, during their declining pore pressure history.

2. Non-linear shear strength, dilation and permeability coupling of joints and fractures is likely to give a more realistic prediction of NFR 4D potential, and of gas-shale stimulation performance, than anything linked to linear Mohr-Coulomb. The over-frequent use of the latter needs a serious review.

3. *Geomechanics* in general and *fracture characterization* in particular, as apparently practiced in the petroleum industry, could usefully be extended into something more resembling rock mechanics practices, where deformation, dilation and coupling with permeability have been of fundamental interest for many decades. This would also now be expected in an industry apparently so dependent on future production from mostly fractured reservoirs.

4. Inevitably there may be impressive ongoing rock mechanics modelling of the non-linear coupled processes discussed in this paper. This may be occurring in some large oil and service companies, or in sponsored university departments. The fact that such work is not readily published or described in workshops means that the present author apologises beforehand to those who cannot easily respond to say ‘we have also been doing that’.

REFERENCES

Bakhtar, K. & Barton, N. [1984] Large scale static and dynamic friction experiments. *Proc. 25th US Rock Mechanics Symp.* Northwestern Univ., Illinois.

Bandis, S., Lumsden, A. & Barton, N. [1981] Experimental studies of scale effects on the shear behaviour of rock joints. *Int. J. of Rock Mech. Min. Sci. and Geomech. Abstr*. 18, 1-21.

Bandis, S., Lumsden, A.C. & Barton, N. [1983] Fundamentals of rock joint deformation. *Int. J. Rock Mech. Min. Sci. and Geomech. Abstr.* 20, 249-268.

Barton, C.A., Zoback, M.D. & Moos, D. [1995] In situ stress and permeability in fractured and faulted crystalline rock. *Mechanics of Jointed and Faulted Rock.*, Rossmanith (Ed.). 381–396. Rotterdam: Balkema.

Barton, N. [1972] A model study of air transport from underground openings situated below groundwater level. Proc. of Symp. of Int. Soc. Rock Mech., *Percolation through fissured rock*, Stuttgart, Theme 3A, 20.

Barton, N. [1973] Review of a new shear strength criterion for rock joints, *Engineering Geology,* Elsevier, Amsterdam, Vol. 7, 287-332.

Barton, N., Lien, R. & Lunde, J. [1974] Engineering classification of rock masses for the design of tunnel support*. Rock Mechanics.* 6: 4: 189-236.

Barton, N. [1976] The shear strength of rock and rock joints. I*nt. Jour. Rock Mech. Min. Sci. and Geomech. Abstr*., Vol. 13, No. 9: 255-279.

Barton, N. & Choubey, V. [1977] The shear strength of rock joints in theory and practice. *Rock Mechanics* 1/2:1-54. Vienna: Springer.

Barton, N. 1981. Hydraulic fracturing to estimate minimum stress and rockmass stability at a pumped hydro project. Proc. of *Workshop on Hydraulic Fracturing Stress Measurements*, Monterey, California.

Barton, N. 1982. Modelling rock joint behaviour from in situ block tests: Implications for nuclear waste repository design. *Office of Nuclear Waste Isolation*, Columbus, OH, 96 p., ONWI-308, September 1982.

Barton, N., Bandis, S. & Bakhtar, K. [1985] Strength, deformation and conductivity coupling of rock joints. *Int. J. Rock Mech. & Min. Sci. & Geomech. Abstr*. 22: 3: 121-140.

Barton, N. [1986] Deformation phenomena in jointed rock. 8th Laurits Bjerrum Memorial Lecture, Oslo. *Geotechnique*, London, Vol. 36: 2: 147-167.

Barton, N., Hårvik, L., Christiansson, M., Bandis, S., Makurat, A., Chryssanthakis, P. & Vik, G. [1986]. Rock mechanics modelling of the Ekofisk reservoir subsidence. Proc. 27th US Rock Mech. Symp., Univ. of Alabama.

Barton, N., Makurat, A., Hårvik, L., Vik, G., Bandis, S., Christianson, M. & Addis, A. [1988] The discontinuum approach to compaction and subsidence modelling as applied to Ekofisk. *BOSS '88. Proc. of Int. Conf. on Behaviour of Offshore Structures*, Trondheim. Vol. 1: 129-141.

Barton, N. [1990] Scale effects or sampling bias? Closing lecture. *Proc. of 1st International Workshop on Scale Effects in Rock Masses,* Loen, Norway. Balkema.

Barton, N. and Quadros, E.F. [1997] Joint aperture and roughness in the prediction of flow and groutability of rock masses. Proc. of NY Rocks '97. Linking Science to Rock Engineering. Ed. K. Kim, 907-916. *Int. J. Rock Mech. and Min. Sci*. Vol. 34: No. 3-4.

Barton, N. [1999] General report concerning some 20th Century lessons and 21st Century challenges in applied rock mechanics, safety and control of the environment. *Proc. of 9th ISRM Congress,* Paris, 3: 1659-1679, Balkema, Netherlands.

Barton, N. [2002] Some new Q-value correlations to assist in site characterization and tunnel design. *Int. J. Rock Mech. & Min. Sci*. Vol. 39/2:185-216.

Barton, N. [2006] *Rock Quality, Seismic Velocity, Attenuation and Anisotropy.* Taylor & Francis, UK & Netherlands, 729 p.

Barton, N. [2007a] Anisotropy and 4D caused by two fracture sets, four compliances, and sheared apertures. *The Leading Edge, SEG,* Sept. 2007, 1112-1117.

Barton, N. [2007b] Fracture-induced seismic anisotropy when shearing is involved in production from fractured reservoirs 12th IWSA, Beijing, 2006. Seismic Anisotropy, Special Issue. Journal of Seismic Exploration, Geophysical Press, Vol. 16, No. 2-4, December 2007.

Barton, N. [2007c] Near-surface gradients of rock quality, deformation modulus, Vp and Qp to 1km depth. First Break, *EAGE*,October, 2007, Vol. 25, 53-60.

Barton, N. and S.K. Pandey, [2011] Numerical modelling of two stoping methods in two Indian mines using degradation of c and mobilization of φ based on Q-parameters. *Int. J. Rock Mech. & Min. Sci.,* Vol. 48, No. 7, 1095-1112.

Barton, N. [2011] From empiricism, through theory, to problem solving in rock engineering. *ISRM Cong., Beijing.* 6th Müller Lecture. Proceedings, Taylor & Francis, Vol. 1, Qian & Zhou (eds), 3-14.

Barton, N. [2013a] Geomechanics and geophysical processes in naturally fractured reservoirs. *2nd. EAGE Workshop on Naturally Fractured Reservoirs*, Muscat, Oman, 33-37.

Barton, N. [2013b] Characterization of fracture shearing for 4D interpretation of fractured reservoirs. *2nd. EAGE Workshop on Naturally Fractured Reservoirs*, Muscat, Oman, 72-76.

Barton, N. [2013c] Shear strength criteria for rock, rock joints, rock fill and rock masses: Problems and some solutions. *Jour. of Rock Mech.and Geotech. Eng., JRMGE* Wuhan, Elsevier, 5(2013) 249-261.

Barton, N. [2014] The shear strength of rock, rock joints, and rock masses: problems and some solutions. *Eurock 2014,* Vigo, Spain. Keynote lecture, 15p.

Byerlee, J. D. [1968] Brittle-ductile transition in rocks. *J. Geophys. Res. 73, 4741-4750.*

Chryssanthakis, P., Monsen, K. & Barton, N. [1991] Validation of UDEC-BB against the CSM block test and large scale application to glacier loading of jointed rock masses. *Proc*. *7th ISRM Cong.*, Aachen. 693–698.

Dusseault, M. [2013] Geomechanical aspects of shale gas development. Keynote lecture, Eurock2013, Wroclow, Poland. *Rock Mechanics for Resources, Energy and Environment. Kwasniewski & Lydzba.* Taylor and Francis, London, p. 39-56.

Fairhurst, C. [2013] Fractures and Fracturing: Hydraulic Fracturing in Jointed Rock. Proc. of Int. Conf. *Effective and Sustainable Hydraulic Fracturing*. An ISRM specialized Conference, Bunger, McLennan, and Jeffrey (editors). Chapter 3, Brisbane, Australia, May 2013.

Fisher, K. and N. Warpinski (2011). Hydraulic Fracture-Height Growth: Real Data *SPE Annual Technical Conference*, Denver, Colorado, USA. SPE 145949, 18p.

Gentier, S.D. [1987] Comportement hydro-mécanique d'une fracture naturelle sous contrainte normale. *Proc. of 6th ISRM Cong. On Rock Mech*., Montréal, Canada, pp. 105-108.

King, G.[2010] Thirty years of gas shale fracturing: what we have learned? SPE 133456. *The SPE Annual Technical Conference and Exhibition, 19-22 September 2010*. Florence, Italy.

Laubach, S.E., Olson, J.E., and Gale, J.F.W., [2004] Are open fractures necessarily aligned with maximum horizontal stress? *Earth & Planetary Science Letters*, v. 222, no. 1, 191-195.

Makurat, A., Barton, N., Rad, N.S. & Bandis, S. [1990] Joint conductivity variation due to normal and shear deformation. *Int. Symp. on Rock Joints.* Loen 1990. Balkema, 535-540.

Makurat, A. & Barton, N. [1988] Rock mechanical computation of deformations and joint apertures during excavation of the Fjellinjen tunnels. Paper 27.1-27.27, *Bergmekanikkdag*, Tapir Press, Oslo 1988.

Mogi, K. [1966] Pressure dependence of rock strength and transition from brittle to ductile flow. *Bull. Earthq. Res. Inst., Tokyo, 44, 215-232.*

Murphy, H. D. and F.C. Fehler [1986] Hydraulic fracturing of jointed formations. SPE 14088, Int. Mtg. on *Petroleum Engineering*, Beijing.

Müller, L. 1966. The progressive failure in jointed media. (in German). *Proc. of ISRM Cong*., Lisbon, 3.74, 679-686.

Nagel, N.B., M. A. Sanchez-Nagel, F. Zhang, X. Garcia & B. Lee [2013] Coupled numerical evaluations of the geomechanical interactions between a hydraulic fracture stimulation and a natural fracture system in shale formations. *Rock Mechanics and Rock Engineering,* Vol. 46, No. 3, 581-609.

Olsson, R. and N. Barton [2001] An improved model for hydro-mechanical coupling during shearing of rock joints. *Int. J. Rock Mech.& Min. Sci.* 38: 317-329. Pergamon.

Pine, R.J. and A.S. Bachelor [1984] Downward migration of shearing in jointed rock during hydraulic injections. *Int. J. Rock Mech. & Min. Sci. Geomech. Abstr.* 21, 5: 249-263.

Price, S. and L. Wei [2013] The relative importance of fracture parameters during fractured reservoir development. *2nd. EAGE Workshop on Naturally Fractured Reservoirs*, Muscat, Oman, 129-134.

Shen, J., R. Jimenez, M. Karakus and C.Xu. [2013] A simplified failure criterion for intact rocks based on rock type and uniaxial compressive strength. *Rock Mech. and Rock Eng*. April, 2013.

Singh, M., Raj, A. and B. Singh [2011] Modified Mohr-Coulomb criterion for non-linear triaxial and polyaxial strength of intact rocks. *Int. J. Rock Mech. Mining Sci.,* 48(4), 546-555.

Zoback, M.D. & Townend, J. [2001] Implications of hydrostatic pore pressures and high crustal strength for the deformation of intraplate lithosphere. *Tectonophysics*, *336*: 19–30.